

# Open-World Continual Learning: Unifying Novelty Detection and Continual Learning

Gyuhak Kim<sup>a,1</sup>, Changnan Xiao<sup>b,1</sup>, Tatsuya Konishi<sup>a,2</sup>, Zixuan Ke<sup>a</sup>, Bing Liu<sup>a,\*</sup>

<sup>a</sup>*University of Illinois at Chicago, 851 S Morgan St, Chicago, Illinois, 60607, United States*

<sup>b</sup>*ByteDance, Building 24, Zone B, 1999 Yishan Road, Shanghai, 201100, China*

---

## Abstract

As AI agents are increasingly used in the real open world with unknowns or novelties, they need the ability to (1) recognize objects that (i) they have learned and (ii) detect items that they have not seen or learned before, and (2) learn the new items incrementally to become more and more knowledgeable and powerful. (1) is called *novelty detection* or *out-of-distribution (OOD) detection* and (2) is called *class incremental learning (CIL)*, which is a setting of *continual learning (CL)*. In existing research, OOD detection and CIL are regarded as two completely different problems. This paper theoretically proves that OOD detection actually is necessary for CIL. We first show that CIL can be decomposed into two sub-problems: *within-task prediction (WP)* and *task-id prediction (TP)*. We then prove that TP is correlated with OOD detection. The *key theoretical result* is that regardless of whether WP and OOD detection (or TP) are defined explicitly or implicitly by a CIL algorithm, good WP and good OOD detection are *necessary* and *sufficient* conditions for good CIL, which unifies novelty or OOD detection and continual learning (CIL, in particular). A good CIL algorithm based on our theory

---

\*Corresponding Author

*Email addresses:* gkim87@uic.edu (Gyuhak Kim), changnanxiao@gmail.com (Changnan Xiao), tt-konishi@kddi.com (Tatsuya Konishi), zke4@uic.edu (Zixuan Ke), liub@uic.edu (Bing Liu)

<sup>1</sup>Equal contribution

<sup>2</sup>The work was done when this author was visiting Bing Liu's group at University of Illinois at Chicago. The original affiliation and address of this author are *KDDI Research, Inc., 2-1-15 Ohara, Fujimino-shi, Saitama, 356-8502, Japan*

*Preprint submitted to Artificial Intelligence*

can naturally be used in open world learning, which is able to perform both novelty/OOD detection and continual learning. Based on the theoretical result, new CIL methods are also designed, which outperform strong baselines in terms of CIL accuracy and its continual OOD detection by a large margin.

*Keywords:* Open world learning, continual learning, OOD detection

---

## 1. Introduction

The current dominant machine learning paradigm (ML) makes the *closed-world assumption*, which means that the classes of objects seen by the system in testing or in deployment must have been seen during training [54, 53, 6, 15, 37], i.e., there is nothing novel occurring during testing or deployment. This assumption is invalid in practice as the real environment is an **open world** that is full of unknowns or novel objects. In order to make an AI agent thrive in the open world, it has to detect novelties and learn them incrementally to make the system more knowledgeable and adaptable over time. This process involves multiple activities, such as *novelty/OOD detection*, *novelty characterization*, *adaption*, *risk assessment*, and *continual learning* of the detected novel items or objects [38]. Novelty detection, also called *out-of-distribution (OOD) detection*, aims to detect unseen objects that the agent has not learned. On detecting the novel objects or situation, the agent has to respond or adapt its actions. But in order to adapt, it must first *characterize* the novel object as without it, the agent would not know how to respond or adapt. For example, it may characterize a detected novel object as looking like a dog. Then, the agent may react like what it would react to a dog. In the process, the agent also constantly assesses the risk of its actions. Finally, it also learns to recognize the new object incrementally so that it will not be surprised when it sees the same kind of object in the future. This incremental learning function is called *continual learning (CL)* or *lifelong learning* [14]. Note that before learning, the agent must obtain labeled training data, which can be collected by the agent through interaction with the environment or with human users. This aspect is out of the scope of this paper. See [38] for details.

This paper focuses only on the key learning aspects of the open world scenario: (1) OOD/novelty detection and (2) continual learning, more specifically *class incremental learning (CIL)* (see the definition below). In the research community, (1) and (2) are regarded as two completely different

problems, but this paper theoretically unifies them by proving that good OOD detection is, in fact, necessary for CIL. Thus, a good CIL algorithm can naturally be used in the open world to perform both (1) and (2). Below, we first define the concepts of OOD detection and continual learning.

***Out-of-distribution (OOD) detection***: Given the training data  $\mathcal{D} = \{(x^i, y^i)_{i=1}^n\}$ , where  $n$  is the number of data samples, and  $x^i \in \mathbf{X}$  is an input sample and  $y^i \in \mathbf{Y}$  (the set of all class labels in  $\mathcal{D}$ ) is its class label, our goal is to build a classifier  $f : \mathbf{X} \rightarrow \mathbf{Y} \cup \{O\}$  that can detect test instances that do not belong to any classes in  $\mathbf{Y}$  (called *OOD detection*), which are assigned to the class  $O$ .  $\mathbf{Y}$  is often called the *in-distribution (IND) classes*.

Note that as we can see from the definition, an OOD detection algorithm can also classify test instances belonging to  $\mathbf{Y}$  to their respective classes, which is called IND classification, although most OOD detection papers do not report the IND classification results.

Continual learning (CL) aims to incrementally learn a sequence of tasks. Each task consists of a set of classes to be learned together (the set may contain only a single class). Once a task is learned, its training data (at least a majority of it) is no longer accessible. Thus, unlike multitask learning, in learning a new task, CL will not be able to use the data of the previous tasks. A major challenge of CL is *catastrophic forgetting (CF)*, which refers to the phenomenon that in learning a new task, the neural network model parameters need to be modified, which may corrupt the knowledge learned for previous tasks in the network and cause performance degradation for the previous tasks [43]. Although a large number of CL techniques have been proposed, they are mainly empirical. Little theoretical work has been done on how to solve CL. This paper performs such a theoretical study about the necessary and sufficient conditions for effective CL. There are two main CL settings that have been extensively studied: *class incremental learning (CIL)* and *task incremental learning (TIL)* [60]. In CIL, the learning process builds a single classifier for all tasks/classes learned so far. In testing, a test instance from any class may be presented for the model to classify. No prior task information (e.g., task-id) of the test instance is provided. Formally, CIL is defined as follows.

***Class incremental learning (CIL)***. CIL learns a sequence of tasks,  $1, 2, \dots, T$ . Each task  $k$  has a training dataset  $\mathcal{D}_k = \{(x_k^i, y_k^i)_{i=1}^{n_k}\}$ , where  $n_k$  is the number of data samples in task  $k$ , and  $x_k^i \in \mathbf{X}$  is an input sample and  $y_k^i \in \mathbf{Y}_k$  (the set of all classes of task  $k$ ) is its class label. All  $\mathbf{Y}_k$ 's are disjoint ( $\mathbf{Y}_k \cap \mathbf{Y}_{k'} = \emptyset, \forall k \neq k'$ ) and  $\bigcup_{k=1}^T \mathbf{Y}_k = \mathbf{Y}$ . The goal of CIL is to construct a

single predictive function or classifier  $f : \mathbf{X} \rightarrow \mathbf{Y}$  that can identify the class label  $y$  of each given test instance  $x$ .

In the TIL setup, each task is a separate or independent classification problem. For example, one task could be to classify different breeds of dog and another task could be to classify different types of animal (the tasks may not be disjoint). One model is built for each task in a shared network. In testing, the task-id of each test instance is provided and the system uses only the specific model for the task (dog or animal classification) to classify the test instance. Formally, TIL is defined as follows.

**Task incremental learning** (TIL). TIL learns a sequence of tasks,  $1, 2, \dots, T$ . Each task  $k$  has a training dataset  $\mathcal{D}_k = \{(x_k^i, k), y_k^i\}_{i=1}^{n_k}$ , where  $n_k$  is the number of data samples in task  $k \in \mathbf{T} = \{1, 2, \dots, T\}$ , and  $x_k^i \in \mathbf{X}$  is an input sample and  $y_k^i \in \mathbf{Y}_k \subset \mathbf{Y}$  is its class label. The goal of TIL is to construct a predictor  $f : \mathbf{X} \times \mathbf{T} \rightarrow \mathbf{Y}$  to identify the class label  $y \in \mathbf{Y}_k$  for  $(x, k)$  (the given test instance  $x$  from task  $k$ ).

This paper focuses on CIL as it incrementally learns new (or novel) classes of objects, which is a core function of open world learning. Although the proposed methods also work for TIL, TIL is not a core part of open world learning as it builds a model for each task separately and independently in a shared neural network and the tasks are given by users. TIL is also much simpler. Several existing techniques can effectively overcome CF for TIL (with almost no CF) [55, 61]. However, CIL remains to be highly challenging due to the additional problem of *Inter-task Class Separation* (ICS), i.e., how to establish decision boundaries between the classes of the new task and the classes of the previous tasks in learning the new tasks without accessing the training data of the previous tasks.

**Problem Statement** (*open-world continual learning* (OCL)): OCL is defined as CIL with the OOD detection capability. At any time, the resulting CIL model is able to classify test instances belonging to the classes learned so far in CIL to their respective classes and also detect OOD instances that do not belong to any of the learned classes so far.

We note that OOD detection in CIL is slightly different from the traditional OOD detection (which sees the full IND data together) because in CIL, the model does not see all the IND data together. In CIL, the IND data comes in a sequence of tasks incrementally and in learning each task, the model does not see any data (or only a very small sample) of the previous tasks.

The main contribution of this paper is two-fold. First, it makes a the-

oretical contribution by proving the necessary and sufficient conditions for solving the CIL problem. It shows that a good OOD detection performance is one of the necessary conditions. Thus, the proposed theory is also applicable to open-world learning as novelty (OOD) detection is a key function of open-world learning and open-world learning should also learn continually, i.e., open-world continual learning. Second, based on the theory, several new CIL algorithms are designed, which are also able to detect novel (or OOD) instances for open-world continual learning (OCL).

**Theory.** We conduct a theoretical study of CIL, which is applicable to any CIL classification model. Instead of focusing on the traditional PAC generalization bound [48] or neural tangent kernel (NTK) [25], we focus on how to solve the CIL problem. We first decompose the CIL problem into two sub-problems in a probabilistic framework: *Within-task Prediction* (WP) and *Task-id Prediction* (TP). WP means that the prediction for a test instance is only done within the classes of the task to which the test instance belongs, which is basically the TIL problem. TP predicts the task-id. TP is needed because in CIL, task-id is not provided in testing. This paper then proves based on the popular cross-entropy loss that (i) the CIL performance is bounded by WP and TP performances, and (ii) TP and task OOD detection performance bound each other (which connects CIL and OOD detection).

**Key theoretical result:** Regardless of whether WP and TP or OOD detection are defined explicitly or implicitly by a CIL algorithm, good WP and good TP or OOD detection are *necessary* and *sufficient* conditions for good CIL performances.<sup>3</sup>

The intuition of the theory is simple because if a CIL model is perfect at detecting OOD samples for each task, which solves the ICS problem, then CIL is reduced to WP, which is just the traditional single-task supervised learning for each task and as indicated earlier, many OOD algorithms can also perform IND classification, which is basically WP.

**New CIL Algorithms for OCL.** The theoretical result provides a principled guidance for solving the CIL problem. Based on the theory, several new CIL methods are designed, including (1) techniques based on the integration of a TIL method and an OOD detection method, which outperforms

---

<sup>3</sup>This result is applicable to both batch/offline and online/stream CIL and to CIL problems with blurry task boundaries which means that some training data of a task may come later together with a future task.

strong baselines in both the CIL and TIL settings by a large margin. This combination is particularly attractive because TIL has achieved no forgetting, and we only need a strong OOD detection technique that can perform both IND prediction and OOD detection to learn each task to achieve strong CIL results. Note that we do not propose a new OOD detection technique as there are numerous such techniques in the literature. We will use two existing ones. (2) Another method is based on a pre-trained model and an OOD replay technique, which performs even better, outperforming existing baselines markedly in both CIL and OOD detection in the OCL setting.

## 2. Related Work

Although a large number of algorithms have been proposed to solve the CIL problem, they are mainly empirical. There are two works that focus on the traditional PAC generalization bound [48] or NTK [25], but they do not tell how to solve the CL problem. This paper focuses on how to solve the CIL problem. To the best of our knowledge, we are not aware of any work that have proposed a theory on how to solve CIL. Also, none of the existing work has connected CIL and OOD detection. Our work shows that a good CIL algorithm can naturally perform OOD detection in the open world. Below, we first survey four popular families in CL approaches, which are mainly for overcoming catastrophic forgetting (CF). We then discuss related works about open world learning.

**(1). Regularization-based methods** prevent forgetting by restricting the learned parameters for previous tasks from being modified significantly by using a regularization term to penalize such changes [29, 68] or regularize the representation or outputs from the previously learned network [35, 69].

**(2). Replay-based methods** [51, 11, 8, 7, 64] prevent forgetting by saving a small amount of training data from previous tasks in a memory buffer and jointly train the network using the current data and the previous task data saved in the memory. Some methods in this family also study which samples in memory should be used in replay [2] or which samples in the training data should be saved for later replay [51, 40].

**(3). Generative methods** construct a generative network to generate raw training data [56, 44, 4]. The generated data are used with the current task training data to jointly train the classification network. [69] generates features instead of raw data. The generated samples in these methods are

used to prevent forgetting in both the generative network and the discriminative network.

**(4). Parameter-isolation methods** [55, 61] train a set of task-specific parameters to effectively protect the important parameters of each task, which thus has almost no forgetting. A limitation of the approach is that the correct task-id of each test instance must be known to the system to select the corresponding task-specific parameters at inference. These methods are thus mainly used for TIL. Some CIL methods also used these methods [1, 45, 49, 22] and they have separate mechanisms to predict the task-id (more on this below). However, their CIL performances are still far below that of recent replay-based counterparts (see Sections 4.2 and 5.2 for details).

Two of our proposed CIL methods use two parameter-isolation methods (HAT [55] and SupSup [61]) for *task incremental learning* (TIL) as one of the components. As mentioned above, some recent CIL approaches have already used TIL methods. In such cases, task-id needs to be predicted. CCG [1] constructs an additional network to predict the task-id. iTAML [49] identifies the task-id of the test data in a batch. A serious limitation of this is that it requires the test data in a batch to belong to the same task. Our methods are different as they can predict (implicitly) for a single test instance at a time. HyperNet [45] and PR [22] propose an entropy based task-id prediction method. SupSup [61] predicts task-id by finding the optimal superpositions at inference. However, these methods perform poorly because they do not know OOD detection is the key for accurate task-id prediction, although our methods do not explicitly predict task-id for each test instance.

*Open world learning* has been studied by many researchers [54, 53, 6, 15, 37, 38]. However, the existing research mainly focused on novelty detection, also called *open set recognition* or *out-of-distribution* (OOD) *detection*. Some researchers have also studied learning the novel objects after they are detected and manually labeled [6, 15, 63, 24]. However, none of them perform continual learning, which has additional challenges of catastrophic forgetting (CF) and inter-task class separation (ICS). Excellent surveys of novelty detection or OOD detection and open world learning can be found in [65, 46, 47, 24]. [17] did novelty detection and also continual learning, but its continual learning uses the regularization based method. It is quite weak because it has serious forgetting. A position paper [31] recently presented some nice blue sky ideas about open world learning, but it does not propose or implement any algorithm.

Our proposed algorithms are quite different. In training, based on our

theory, we use two existing OOD detection methods to verify that our theory can guide us to design new and much more effective CIL algorithms. In testing, our OOD detection is in the open-world continual learning (OCL) setting, which has been described in the introduction section.

There are also several papers that study *novel class discovery* [18], which is defined as discovering the hidden classes in the detected novel or OOD instances. Our work does not perform this function. We assume that the training data for each new task is given. Performing automatic class label discovery is still very challenging as in many cases, the class assignments can be subjective and are determined by human users. For example, for a dog, whether it should just be labeled as dog or a specific breed of dog is a subjective decision and is depending on applications.

### 3. A Theoretical Study on Solving CIL

This section presents our theory for solving CIL, which also covers novelty or OOD detection in the open world. It first shows that the CIL performance improves if the within-task prediction (WP) performance and/or the task-id prediction (TP) performance improve, and then shows that TP and OOD detection bound each other, which indicates that CIL performance is controlled by WP and OOD detection. This connects CIL and OOD detection. Finally, we study the necessary conditions for a good CIL model, which includes a good WP, and a good TP or OOD detection.

#### 3.1. CIL Problem Decomposition

This sub-section first presents the assumptions made by CIL based on its definition and then proposes a decomposition of the CIL problem into two sub-problems. A CIL system learns a sequence of tasks  $\{(\mathbf{X}_k, \mathbf{Y}_k)\}_{k=1,\dots,T}$ , where  $\mathbf{X}_k$  is the domain of task  $k$  and  $\mathbf{Y}_k$  are classes of task  $k$  as  $\mathbf{Y}_k = \{\mathbf{Y}_{k,j}\}$ , where  $j$  indicates the  $j$ th class in task  $k$ . Let  $\mathbf{X}_{k,j}$  to be the domain of  $j$ th class of task  $k$ , where  $\mathbf{X}_k = \bigcup_j \mathbf{X}_{k,j}$ . For accuracy, we will use  $x \in \mathbf{X}_{k,j}$  instead of  $\mathbf{Y}_{k,j}$  in probabilistic analysis. Based on the definition of class incremental learning (CIL) (Section 1), the following assumptions are implied,

**Assumption 1.** The domains of classes of the same task are disjoint, i.e.,  $\mathbf{X}_{k,j} \cap \mathbf{X}_{k,j'} = \emptyset, \forall j \neq j'$ .

**Assumption 2.** The domains of tasks are disjoint, i.e.,  $\mathbf{X}_k \cap \mathbf{X}_{k'} = \emptyset, \forall k \neq k'$ .



For any ground event  $D$ , the goal of a CIL problem is to learn  $\mathbf{P}(x \in \mathbf{X}_{k,j}|D)$ . This can be decomposed into two probabilities, *within-task IND prediction* (WP) probability and *task-id prediction* (TP) probability. WP probability is  $\mathbf{P}(x \in \mathbf{X}_{k,j}|x \in \mathbf{X}_k, D)$  and TP probability is  $\mathbf{P}(x \in \mathbf{X}_k|D)$ . We can rewrite the CIL problem using WP and TP based on the two assumptions,

$$\mathbf{P}(x \in \mathbf{X}_{k_0,j_0}|D) = \sum_{k=1,\dots,n} \mathbf{P}(x \in \mathbf{X}_{k,j_0}|x \in \mathbf{X}_k, D)\mathbf{P}(x \in \mathbf{X}_k|D) \quad (1)$$

$$= \mathbf{P}(x \in \mathbf{X}_{k_0,j_0}|x \in \mathbf{X}_{k_0}, D)\mathbf{P}(x \in \mathbf{X}_{k_0}|D) \quad (2)$$

where  $k_0$  means a particular task and  $j_0$  a particular class in the task.

Some remarks are in order about Eq. 2 and our subsequent analysis to set the stage.

*Remark 1.* Eq. 2 shows that if we can improve either the WP or TP performance, or both, we can improve the CIL performance.

*Remark 2.* It is important to note that our theory is not concerned with the learning algorithm or training process. But we will propose some concrete CIL algorithms based on the theoretical result in the experiment section.

*Remark 3.* Note that the CIL definition and the subsequent analysis are applicable to tasks with any number of classes (including only one class per task) and to online CIL where the training data for each task or class comes gradually in a data stream and may also cross task boundaries (blurry tasks [5]) because our analysis is based on an already-built CIL model after training. Regarding blurry task boundaries, suppose dataset 1 has classes {dog, cat, tiger} and dataset 2 has classes {dog, computer, car}. We can define task 1 as {dog, cat, tiger} and task 2 as {computer, car}. The shared class *dog* in dataset 2 is just additional training data of *dog* appeared after task 1.

*Remark 4.* Furthermore,  $\text{CIL} = \text{WP} * \text{TP}$  in Eq. 2 means that when we have WP and TP (defined either explicitly or implicitly by implementation), we can find a corresponding CIL model defined by  $\text{WP} * \text{TP}$ . Similarly, when we have a CIL model, we can find the corresponding underlying WP and TP defined by their probabilistic definitions.

In the following sub-sections, we develop this further concretely to derive the sufficient and necessary conditions for solving the CIL problem in the context of cross-entropy loss as it is used in almost all supervised CIL systems.

### 3.2. CIL Improves as WP and/or TP Improve

As stated in Remark 2 above, the study here is based on a *trained CIL model* and not concerned with the algorithm used in training the model. We use cross-entropy as the performance measure of a trained model as it is the most popular loss function used in supervised CL. For experimental evaluation, we use *accuracy* following CL papers. Denote the cross-entropy of two probability distributions  $p$  and  $q$  as

$$H(p, q) \stackrel{def}{=} -\mathbb{E}_p[\log q] = -\sum_i p_i \log q_i. \quad (3)$$

For any  $x \in \mathbf{X}$ , let  $y$  to be the CIL ground truth label of  $x$ , where  $y_{k_0, j_0} = 1$  if  $x \in \mathbf{X}_{k_0, j_0}$  otherwise  $y_{k, j} = 0, \forall (k, j) \neq (k_0, j_0)$ . Let  $\tilde{y}$  be the WP ground truth label of  $x$ , where  $\tilde{y}_{k_0, j_0} = 1$  if  $x \in \mathbf{X}_{k_0, j_0}$  otherwise  $\tilde{y}_{k_0, j} = 0, \forall j \neq j_0$ . Let  $\bar{y}$  be the TP ground truth label of  $x$ , where  $\bar{y}_{k_0} = 1$  if  $x \in \mathbf{X}_{k_0}$  otherwise  $\bar{y}_k = 0, \forall k \neq k_0$ . Denote

$$H_{WP}(x) = H(\tilde{y}, \{\mathbf{P}(x \in \mathbf{X}_{k_0, j} | x \in \mathbf{X}_{k_0}, D)\}_j), \quad (4)$$

$$H_{CIL}(x) = H(y, \{\mathbf{P}(x \in \mathbf{X}_{k, j} | D)\}_{k, j}), \quad (5)$$

$$H_{TP}(x) = H(\bar{y}, \{\mathbf{P}(x \in \mathbf{X}_k | D)\}_k) \quad (6)$$

where  $H_{WP}$ ,  $H_{CIL}$  and  $H_{TP}$  are the cross-entropy values of WP, CIL and TP, respectively. We now present our first theorem. The theorem connects CIL to WP and TP, and suggests that by having a good WP or TP, the CIL performance improves as the upper bound for the CIL loss decreases.

**Theorem 1.** *If  $H_{TP}(x) \leq \delta$  and  $H_{WP}(x) \leq \epsilon$ , we have  $H_{CIL}(x) \leq \epsilon + \delta$ .*

The detailed proof is given in Appendix A.1. This theorem holds regardless of whether WP and TP are trained together or separately. When they are trained separately, if WP is fixed and we let  $\epsilon = H_{WP}(x)$ ,  $H_{CIL}(x) \leq H_{WP}(x) + \delta$ , which means if TP is better, CIL is better. Similarly, if TP is fixed, we have  $H_{CIL}(x) \leq \epsilon + H_{TP}(x)$ . When they are trained concurrently, there exists a functional relationship between  $\epsilon$  and  $\delta$  depending on implementation. But no matter what it is, when  $\epsilon + \delta$  decreases, CIL gets better.

Theorem 1 holds for any  $x \in \mathbf{X} = \bigcup_k \mathbf{X}_k$  that satisfies  $H_{TP}(x) \leq \delta$  or  $H_{WP}(x) \leq \epsilon$ . To measure the overall performance under expectation, we present the following corollary.

**Corollary 1.** *Let  $U(\mathbf{X})$  represents the uniform distribution on  $\mathbf{X}$ . i) If  $\mathbb{E}_{x \sim U(\mathbf{X})}[H_{TP}(x)] \leq \delta$ , then  $\mathbb{E}_{x \sim U(\mathbf{X})}[H_{CIL}(x)] \leq \mathbb{E}_{x \sim U(\mathbf{X})}[H_{WP}(x)] + \delta$ . Similarly, ii)  $\mathbb{E}_{x \sim U(\mathbf{X})}[H_{WP}(x)] \leq \epsilon$ , then  $\mathbb{E}_{x \sim U(\mathbf{X})}[H_{CIL}(x)] \leq \epsilon + \mathbb{E}_{x \sim U(\mathbf{X})}[H_{TP}(x)]$ .*

The proof is given in Appendix A.2. The corollary is a direct extension of Theorem 1 in expectation. The implication is that given TP performance, CIL is positively related to WP. The better the WP is, the better the CIL is as the upper bound of the CIL loss decreases. Similarly, given WP performance, a better TP performance results in a better CIL performance. Due to the positive relation, we can improve CIL by improving either WP or TP using their respective methods developed in each area.

### 3.3. Task Prediction (TP) to OOD Detection

Building on Eq. 2, we have studied the relationship of CIL, WP and TP in Theorem 1. We now connect TP and OOD detection. They are shown to be dominated by each other to a constant factor.

We again use cross-entropy  $H$  to measure the performance of TP and OOD detection of a trained network as in Section 3.2. To build the connection between  $H_{TP}(x)$  and OOD detection of each task, we first define the notations of OOD detection. We use  $\mathbf{P}'_k(x \in \mathbf{X}_k|D)$  to represent the probability distribution predicted by the  $k$ th task's OOD detector. Notice that the task prediction (TP) probability distribution  $\mathbf{P}(x \in \mathbf{X}_k|D)$  is a categorical distribution over  $T$  tasks, while the OOD detection probability distribution  $\mathbf{P}'_k(x \in \mathbf{X}_k|D)$  is a Bernoulli distribution. For any  $x \in \mathbf{X}$ , define

$$H_{OOD,k}(x) = \begin{cases} H(1, \mathbf{P}'_k(x \in \mathbf{X}_k|D)) = -\log \mathbf{P}'_k(x \in \mathbf{X}_k|D), & x \in \mathbf{X}_k, \\ H(0, \mathbf{P}'_k(x \in \mathbf{X}_k|D)) = -\log \mathbf{P}'_k(x \notin \mathbf{X}_k|D), & x \notin \mathbf{X}_k. \end{cases} \quad (7)$$

In CIL, the OOD detection probability for a task can be defined using the output values corresponding to the classes of the task. Some examples of the function is a sigmoid of maximum logit value or a maximum softmax probability after re-scaling to 0 to 1. It is also possible to define the OOD detector directly as a function of tasks instead of a function of the output values of all classes of tasks, i.e. Mahalanobis distance. The following theorem shows that TP and OOD detection bound each other.

**Theorem 2.** *i) If  $H_{TP}(x) \leq \delta$ , let  $\mathbf{P}'_k(x \in \mathbf{X}_k|D) = \mathbf{P}(x \in \mathbf{X}_k|D)$ , then  $H_{OOD,k}(x) \leq \delta, \forall k = 1, \dots, T$ . ii) If  $H_{OOD,k}(x) \leq \delta_k, k = 1, \dots, T$ , let  $\mathbf{P}(x \in \mathbf{X}_k|D) = \frac{\mathbf{P}'_k(x \in \mathbf{X}_k|D)}{\sum_k \mathbf{P}'_k(x \in \mathbf{X}_k|D)}$ , then  $H_{TP}(x) \leq (\sum_k \mathbf{1}_{x \in \mathbf{X}_k} e^{\delta_k})(\sum_k 1 - e^{-\delta_k})$ , where  $\mathbf{1}_{x \in \mathbf{X}_k}$  is an indicator function.*

See Appendix A.3 for the proof. As we use cross-entropy, the lower the bound, the better the performance is. The first statement (i) says that the OOD detection performance improves if the TP performance gets better (i.e., lower  $\delta$ ). Similarly, the second statement (ii) says that the TP performance improves if the OOD detection performance on each task improves (i.e., lower  $\delta_k$ ). Besides, since  $(\sum_k \mathbf{1}_{x \in \mathbf{X}_k} e^{\delta_k})(\sum_k 1 - e^{-\delta_k})$  converges to 0 as  $\delta_k$ 's converge to 0 in order of  $O(|\sum_k \delta_k|)$ , we further know that  $H_{TP}$  and  $\sum_k H_{OOD,k}$  are equivalent in quantity up to a constant factor.

In Theorem 1, we studied how CIL is related to WP and TP. In Theorem 2, we showed that TP and OOD bound each other. Now we explicitly give the upper bound of CIL in relation to WP and OOD detection of each task. The detailed proof can be found in Appendix A.4.

**Theorem 3.** *If  $H_{OOD,k}(x) \leq \delta_k$ ,  $k = 1, \dots, T$  and  $H_{WP}(x) \leq \epsilon$ , we have*

$$H_{CIL}(x) \leq \epsilon + \left( \sum_k \mathbf{1}_{x \in \mathbf{X}_k} e^{\delta_k} \right) \left( \sum_k 1 - e^{-\delta_k} \right),$$

where  $\mathbf{1}_{x \in \mathbf{X}_k}$  is an indicator function.

### 3.4. Necessary Conditions for Improving CIL

In Theorem 1, we showed that good performances of WP and TP are sufficient to guarantee a good performance of CIL. In Theorem 3, we showed that good performances of WP and OOD are sufficient to guarantee a good performance of CIL. For completeness, we study the necessary conditions of a well-performed CIL in this sub-section.

**Theorem 4.** *If  $H_{CIL}(x) \leq \eta$ , then there exist i) a WP, s.t.  $H_{WP}(x) \leq \eta$ , ii) a TP, s.t.  $H_{TP}(x) \leq \eta$ , and iii) an OOD detector for each task, s.t.  $H_{OOD,k} \leq \eta$ ,  $k = 1, \dots, T$ .*

The detailed proof is given in Appendix A.5. This theorem tells that if a good CIL model is trained, then a good WP, a good TP and a good OOD detector for each task are always implied. More importantly, by transforming Theorem 4 into its contraposition, we have the following statements: If for any WP,  $H_{WP}(x) > \eta$ , then  $H_{CIL}(x) > \eta$ . If for any TP,  $H_{TP}(x) > \eta$ , then  $H_{CIL}(x) > \eta$ . If for any OOD detector,  $H_{OOD,k}(x) > \eta$ ,  $k = 1, \dots, T$ , then  $H_{CIL}(x) > \eta$ . Regardless of whether WP and TP (or OOD detection) are defined explicitly or implicitly by a CIL algorithm, the existence of a good WP and the existence of a good TP or OOD detection are necessary conditions for a good CIL performance.

*Remark 5.* It is important to note again that our study in this section is based on a CIL model that has already been built. In other words, our study tells the CIL designers what should be achieved in the final model. Clearly, one would also like to know how to design a strong CIL model based on the theoretical results, which also considers catastrophic forgetting (CF). One effective method is to make use of a strong existing TIL algorithm, which can already achieve no or little forgetting (CF), and combine it with a strong OOD detection algorithm (as mentioned earlier, most OOD detection methods can also perform WP). Thus, any improved method from the OOD detection community can be applied to CIL to produce improved CIL systems (see Sections 4.2.3 and 4.2.4).

Recall in Section 2, we reviewed prior works that have tried to use a TIL method for CIL with a task-id prediction method [45, 3, 49, 1, 22]. However, since they did not know that the key to the success of this approach is a strong OOD detection algorithm, they are quite weak (see Sections 4.2 and 5.2).

*Remark 6.* Since good OOD detection for each task is necessary for CIL, our theory thus covers novelty (OOD) detection for open world learning.

#### 4. Proposed Approach 1: Combining TIL and OOD Detection

Based on the above theoretical result, we designed two approaches (three different methods) to solve CIL that employ OOD detection. One more method will also be discussed in Section 4.2, which is a weaker post-processing OOD detection technique. This section presents the first approach, which combines a task incremental learning (TIL) method and an OOD detection method. The approach does not save any training data from previous tasks. In the next section, we present the second approach, which is based on replay and needs to save some training data from previous tasks.

##### 4.1. Combining a TIL Method and an OOD Detection Method

As mentioned earlier, several existing TIL methods can overcome CF. This proposed approach basically leverages the CF prevention ability in two TIL methods (HAT [55] and SupSup (Sup) [61]) and replaces their task learning methods with an OOD detection technique, called CSI [58], which can perform both within-task or IND prediction (WP) and OOD instance detection. Below, we first introduce the two TIL methods, HAT and SupSup, and the OOD detection method, CSI. The combinations give two new CIL

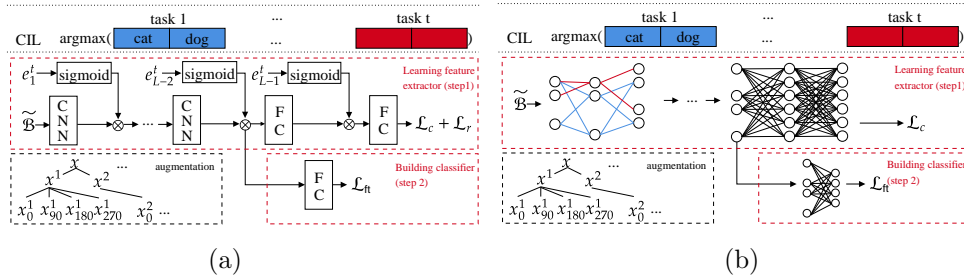


Figure 1: Overview of prediction and training framework of HAT+CSI and Sup+CSI. **(a)** HAT+CSI: The CIL prediction is made by argmax over the concatenated output from each task. The training of each task uses CSI. That is, the training batch is augmented to give different views of the samples for contrastive training. The training consists of two steps following CSI. The first step learns the feature extractor by using the hard attention algorithm [55], which applies task embeddings to find hard masks at each layer. Then given the learned feature representations, it fine-tunes the classifier in step 2. **(b)** Sup+CSI: The CIL prediction is also made by taking argmax over the concatenated output values from each task as HAT+CSI. The model training for each task is similar to HAT+CSI except that it uses the Edge Popup algorithm of SupSup [50] to find a sparse network for each task. The sparse networks, which are indicated by edges of different colors in the diagram. The second step fine-tunes the classifier only with the fixed feature extractor.

methods, HAT+CSI and Sup+CSI. None of these methods needs to save any data from previous tasks.

Figure 1 shows the overall training frameworks of HAT+CSI and Sup+CSI. Note that both HAT and Sup are multi-head methods (one head for each task) designed for task incremental learning (TIL).

#### 4.1.1. HAT: Hard Attention Masks

To prevent forgetting of the trained OOD detection model  $f^k \circ h^k$  for each task  $k$  in subsequent task learning, the hard attention mask (HAT) [55] for TIL is employed (which prevents forgetting in the feature extractor). Specifically, in learning a task, a set of embeddings are trained to protect the important neurons so that the corresponding parameters are not interfered by subsequent tasks. The importance of a neuron is measured by the 0-1 pseudo-step function, where 0 indicates not important and 1 indicates important (and thus protected).

The hard attention mask is an output of sigmoid function  $u$  with a hyper-

parameter  $s$

$$a_l^k = u(se_l^k), \quad (8)$$

where  $e_l^k$  is a learnable embedding at layer  $l$  of task  $k$ . Since the step function is not differentiable, a sigmoid function with a large  $s$  is used to approximate it. Sigmoid is approximately a 0-1 step function with a large  $s$ . The attention is multiplied to the output  $h_l = \text{ReLU}(W_l h_{l-1} + b_l)$  of layer  $l$ ,

$$h'_l = a_l^k \otimes h_l \quad (9)$$

The  $j$ th element  $a_{j,l}^k$  in the attention mask blocks (or unblocks) the information flow from neuron  $j$  at layer  $l$  if its value is 0 (or 1). With 0 value of  $a_{j,l}^k$ , the corresponding parameters in  $W_l$  and  $b_l$  can be freely changed as the output values  $h'_l$  are not affected. The neurons with non-zero mask values are necessary to perform the task, and thus need a protection for catastrophic forgetting.

We modify the gradients of parameters that are important in performing the previous tasks  $(1, \dots, k-1)$  during training task  $k$  so they are not interfered. Denote the accumulated mask by

$$a_l^{<k} = \max(a_l^{<k-1}, a_l^{k-1}) \quad (10)$$

where  $\max$  is element-wise maximum and the initial mask  $a_l^0$  is a zero vector. It is a collection of mask values at layer  $l$  where a neuron has value 1 if it has ever been activated previously. The gradient of parameter  $w_{ij,l}$  is modified as

$$\nabla w'_{ij,l} = (1 - \min(a_{i,l}^{<k}, a_{j,l-1}^{<k})) \nabla w_{ij,l} \quad (11)$$

where  $a_{i,l}^{<k}$  is the  $i$ th unit of  $a_l^{<k}$ . The gradient flow is blocked if both neurons  $i$  in the current layer and  $j$  in the previous layer have been activated. We apply the mask for all layers except the last layer. The parameters in last layer do not need to be protected as they are task-specific parameters.

A regularization is introduced to encourage sparsity in  $a_l^k$  and parameter sharing with  $a_l^{<k}$ . The capacity of a network depletes when  $a_l^{<k}$  becomes 1-vector in all layers. Despite a set of new neurons can be added in network at any point in training for more capacity, we utilize resources more efficiently by minimizing the loss

$$\mathcal{L}_r = \lambda \frac{\sum_l \sum_i a_{i,l}^k (1 - a_{i,l}^{<k})}{\sum_l \sum_i (1 - a_{i,l}^{<k})} \quad (12)$$

where  $\lambda$  is a hyper-parameter. The final objective to train a comprehensive task network without forgetting is

$$\mathcal{L} = \mathcal{L}_{ce} + \mathcal{L}_r \quad (13)$$

where  $\mathcal{L}_{ce}$  is the cross-entropy loss. The overall framework of the algorithm is shown in Figure 1(a).

Note that for TIL, HAT needs the task-id for each test instance in order to choose the right task model for prediction or classification. However, by replacing the original model building method for each task in HAT with the OOD detection method in CSI (more specifically,  $\mathcal{L}_c$ ) during training, HAT+CSI does not require to know the task-id of each test instance at inference, which makes HAT+CSI suitable for CIL (class incremental learning). We will see the detailed prediction/classification method in Section 4.2.

#### 4.1.2. SupSup: Supermasks in Superposition

SupSup (Sup) [61] is also a highly effective method that can overcome forgetting in the TIL setting. Sup trains supermasks by Edge Popup algorithm in [50]. More precisely, given initial  $\mathbf{W}$ , find binary masks  $\mathbf{M}_k$  for task  $k$  to minimize the cross-entropy loss

$$\mathcal{L} = -\frac{1}{|\mathbf{X}_k|} \sum \log p(y|x, k), \quad (14)$$

where  $\mathbf{X}_k$  is the training data for task  $k$ , and

$$p(y|x, k) = f(h(x; \mathbf{W} \otimes \mathbf{M}_k)), \quad (15)$$

where  $\otimes$  indicates element-wise product. The masks are obtained by selecting the top  $p\%$  of entries in the score matrices  $\mathbf{V}$ . The  $p$  value determines the sparsity of the mask  $\mathbf{M}_k$ . The subnetwork found by Edge Popup algorithm is indicated by different colors in Figure 1(b).

Like HAT, Sup is also for TIL and needs the task-id  $k$  of each test instance at inference. With  $k$ , the system (which is referred to as Sup GG in the original Sup paper) uses the task-specific mask  $\mathbf{M}_k$  to obtain the classification output. Like HAT+CSI, by replacing the cross-entropy loss in mask finding with the OOD detection loss in CSI, Sup+CSI also does not require the task-id of each test instance, which makes Sup+CSI applicable to CIL (class incremental learning). We will discuss the detailed prediction/classification method in Section 4.2.



#### 4.1.3. CSI: Contrasting Shifted Instances for OOD Detection

We now explain the OOD detection method CSI. CSI is based on contrastive learning [13, 27] and data and class augmentations due to their excellent performance [58]. Since here we focus on how to learn a single task based on OOD detection, we omit the task-id unless necessary. The OOD training process is similar to that of contrastive learning. It consists of two steps: Step 1 learns the feature representation by the composite  $g \circ h$ , where  $h$  is the feature extractor and  $g$  is the projection to contrastive representation, and Step 2 learns/fine-tunes the linear classifier  $f$ , mapping the feature representation of  $h$  to the label space (the classifier is the OOD model). This two-step training process is outlined in Figure 1(b). In the following, we first describe the two-step training process and then explain how to make a prediction based on an ensemble method to further improve prediction.

**Step 1 (Contrastive Loss for Feature Learning).** Supervised contrastive learning is used to try to repel data of different classes and align data of the same class more closely to make it easier to classify them. A key operation is data augmentation via transformations.

Given a batch of  $N$  samples, each sample  $x$  is first duplicated. Each version then goes through *three initial augmentations* (horizontal flip, color changes, and Inception crop [57]) to generate two different views  $x^1$  and  $x^2$  (they keep the same class label as  $x$ ). Denote the augmented batch by  $\mathcal{B}$ , which now has  $2N$  samples. In [21] and [58], it was shown that using image rotations is effective in learning OOD detection models because such rotations can effectively serve as out-of-distribution (OOD) training data. For each augmented sample  $x \in \mathcal{B}$  with class  $y$  of a task, we rotate  $x$  by  $90^\circ, 180^\circ, 270^\circ$  to create three images, which are assigned *three new classes*  $y_1, y_2,$  and  $y_3$ , respectively. This results in a larger augmented batch  $\tilde{\mathcal{B}}$ . Since we generate three new images from each  $x$ , the size of  $\tilde{\mathcal{B}}$  is  $8N$ . For each original class, we now have 4 classes. For a sample  $x \in \tilde{\mathcal{B}}$ , let  $\tilde{\mathcal{B}}(x) = \tilde{\mathcal{B}} \setminus \{x\}$  and let  $P(x) \subset \tilde{\mathcal{B}} \setminus \{x\}$  be a set consisting of the data of the same class as  $x$  distinct from  $x$ . The contrastive representation of a sample  $x$  is  $z_x = g(h(x, k)) / \|g(h(x, k))\|$ , where  $k$  is the current task. In learning, we minimize the supervised contrastive loss.

$$\mathcal{L}_c = \frac{1}{8N} \sum_{x \in \tilde{\mathcal{B}}} \frac{-1}{|P(x)|} \sum_{p \in P(x)} \log \frac{\exp(z_x \cdot z_p / \tau)}{\sum_{x' \in \tilde{\mathcal{B}}(x)} \exp(z_x \cdot z_{x'} / \tau)}, \quad (16)$$

where  $\tau$  is a scalar temperature,  $\cdot$  is dot product, and  $\times$  is multiplication.

The loss is reduced by repelling  $z$  of different classes and aligning  $z$  of the same class more closely.  $\mathcal{L}_c$  basically trains a feature extractor with good representations for learning an OOD classifier.

Since the feature extractor is shared across tasks in continual learning, a protection is needed to prevent catastrophic forgetting. HAT and Sup use their respective techniques to protect their feature extractor from forgetting. Therefore, the losses  $\mathcal{L}$  of Eq. 14 and  $\mathcal{L}_{ce}$  of Eq. 13 are replaced by Eq. 16 while the forgetting prevention mechanisms still hold.

**Step 2 (Fine-tuning the Classifier).** Given the feature extractor  $h$  trained with the loss in Eq. 16, we *freeze*  $h$  and only *fine-tune* the linear classifier  $f$ , which is trained to predict the classes of task  $k$  and the augmented rotation classes.  $f$  maps the feature representation to the label space in  $\mathcal{R}^{4|\mathcal{C}^k|}$ , where 4 is the number of rotation classes including the original data with  $0^\circ$  rotation and  $|\mathcal{C}^k|$  is the number of original classes in task  $k$ . We minimize the cross-entropy loss,

$$\mathcal{L}_{\text{ft}} = -\frac{1}{|\tilde{\mathcal{B}}|} \sum_{(x,y) \in \tilde{\mathcal{B}}} \log \tilde{p}(y|x, k), \quad (17)$$

where ft indicates fine-tune, and

$$\tilde{p}(y|x, k) = \text{softmax}(f(h(x, k))) \quad (18)$$

where  $f(h(x, k)) \in \mathcal{R}^{4|\mathcal{C}^k|}$ . The output  $f(h(x, k))$  includes the rotation classes. The linear classifier is trained to predict the original and the rotation classes. Since individual classifier is trained for each task and the feature extractor is frozen, no protection is necessary.

**Ensemble Class Prediction.** We now discuss the prediction of class label  $y$  for a test sample  $x$ . Note that the network  $f \circ h$  in Eq. 18 returns logits for rotation classes (including the original task classes). Note also for each original class label  $j_k \in \mathcal{C}^k$  (original classes) of a task  $k$ , we created three additional rotation classes. For class  $j_k$ , the classifier  $f$  will produce four output values from its four rotation class logits, i.e.,  $f_{j_k,0}(h(x_0, k))$ ,  $f_{j_k,90}(h(x_{90}, k))$ ,  $f_{j_k,180}(h(x_{180}, k))$ , and  $f_{j_k,270}(h(x_{270}, k))$ , where 0, 90, 180, and 270 represent  $0^\circ$ ,  $90^\circ$ ,  $180^\circ$ , and  $270^\circ$  rotations respectively and  $x_0$  is the original  $x$ . We compute an ensemble output  $f_{j_k}(h(x))$  for each class  $j_k \in \mathcal{C}^k$  of task  $k$ ,

$$f(h(x, k))_{j_k} = \frac{1}{4} \sum_{\text{deg}} f(h(x_{\text{deg}}, k))_{j_k, \text{deg}}. \quad (19)$$

## 4.2. Experiments

We now present the experimental results of the combination techniques HAT+CSI and Sup+CSI for *class incremental learning* (CIL). We will also use another OOD detection method ODIN [36] to show that better OOD detection method leads to better CIL results. We do not conduct extensive experiments on ODIN as it is much weaker than CSI in terms of OOD detection. Note that we will not report the OOD detection results for HAT+CSI and Sup+CSI in the open world in the continual learning process as the proposed method MORE in the next section performs better.

### 4.2.1. Experimental Datasets and Baselines

**Datasets and CIL tasks:** We use three standard image classification benchmark datasets and construct five different CIL experiments.

(1). **CIFAR-10** [30]: This dataset consists of 32x32 color images of 10 classes with 50,000 training and 10,000 testing samples. We construct an experiment (**C10-5T**) of 5 tasks with 2 classes per task.

(2). **CIFAR-100** [30]: This dataset consists of 32x32 color images of 100 classes with 50,000 training and 10,000 testing samples. We construct two experiments of 10 tasks (**C100-10T**) and 20 tasks (**C100-20T**), where each task has 10 classes and 5 classes, respectively.

(3). **Tiny-ImageNet** [32]: This is an image classification dataset with 64x64 color images of 200 classes with 100,000 training and 10,000 validation samples. Since the dataset does not provide labels for testing data, we use the validation data for testing. We construct two experiments of 5 tasks (**T-5T**) and 10 tasks (**T-10T**) with 40 classes per task and 20 classes per task, respectively.

**Baselines:** We use 18 diverse continual learning baselines:

- (1). One projection method (**OWM** [67]).
- (2). Two exemplar-free (no replay data is saved) regularization methods (**MUC** [39] and **PASS** [69]).
- (3). Nine replay-based methods (**LwF** [35], **iCaRL** [51], **A-GEM** [11], **EEIL** [8], **GD** [34], **Mnemonics** [40], **BiC** [62], **DER++** [7], and **HAL** [10]).
- (4). Three parameter-isolation methods (**HAT** [55], **HyperNet** [45], and **SupSup** [61]).
- (5). Additionally, we report the accuracies of replay-based method **Co<sup>2</sup>L** [9] and parameter isolation methods **CCG** [1] and **PR-Ent** [22] from their

original papers as CCG has not released the code and we are unable to run Co<sup>2</sup>L and PR-Ent on our machines.

#### 4.2.2. Training Details and Evaluation Metrics

**Training Details.** For the backbone structure, we follow [61, 69, 7] and use ResNet-18 [19]. For CIFAR-100 and Tiny-ImageNet, the number of channels are doubled to fit more classes. For all baselines, the same ResNet-18 backbone architecture is employed except for OWM and HyperNet, for which we use their original architectures. OWM uses AlexNet. It is not obvious how to apply its orthogonal projection technique to the ResNet structure. HyperNet uses ResNet-32 and we are unable to replace it due to model initialization arguments unexplained in the original paper. For the replay methods, we use memory buffer 200 for CIFAR-10 and 2000 for CIFAR-100 and Tiny-ImageNet as in [51, 7]. We use the hyper-parameters suggested by the authors. If we could not reproduce any result, we use 10% of the training data as a validation set to grid-search for good hyper-parameters. For our proposed methods, we report the hyper-parameters in Appendix F. All the results are averages over 5 runs with random seeds.

#### Evaluation Metrics.

(1). *Average classification accuracy* over all classes after learning the last task. The final class prediction depends *prediction methods* (see below). We also report *forgetting rate* in Appendix G.

(2). *Average AUC* (Area Under the ROC Curve) over all task models for the evaluation of OOD detection. AUC is the main measure used in OOD detection papers. Using this measure, we show that a better OOD detection method will result in a better CIL performance. Let  $AUC_k$  be the AUC score of task  $k$ . It is computed by using only the model (or classes) of task  $k$  to score the test data of task  $k$  as the in-distribution (IND) data and the test data from other tasks as the out-of-distribution (OOD) data. The average AUC score is:  $AUC = \sum_k AUC_k/n$ , where  $n$  is the number of tasks.

It is not straightforward to change existing CL algorithms to include a new OOD detection method that needs training, e.g., CSI, except for TIL (task incremental learning) methods like HAT and Sup. For HAT and Sup, we can simply switch their methods for learning each task with CSI (see Section 4.1.1 and Section 4.1.2).

**Prediction Methods.** The theoretical result in Section 3 states that we use Eq. 2 to perform the final prediction. The first probability (WP) in Eq. 2 is easy to get as we can simply use the softmax values of the classes in

each task. However, the second probability (TP) in Eq. 2 is tricky as each task is learned without the data of other tasks. There can be many options. We take the following approaches for prediction (which are a special case of Eq. 2, see below):

(1). For those approaches that use a single classification head to include all classes learned so far, we predict as follows (which is also the approach taken by the existing papers.)

$$\hat{y} = \arg \max f(x) \quad (20)$$

where  $f(x)$  is the logit output of the network.

(2). For multi-head methods (e.g., HAT, HyperNet, and Sup), which use one head for each task, we use the concatenated output as

$$\hat{y} = \arg \max \bigoplus_k f(x)_k \quad (21)$$

where  $\bigoplus$  indicate concatenation and  $f(x)_k$  is the output of task  $k$ .<sup>4</sup>

These methods (in fact, they are the same method used in two different settings) are a special case of Eq. 2 if we define  $OOD_k$  as  $\sigma(\max f(x)_k)$ , where  $\sigma$  is the sigmoid. Hence, the theoretical results in Section 3 are still applicable. We present a detailed explanation about this prediction method and some other options in Appendix C. These two approaches work quite well.

#### 4.2.3. Better OOD Detection Produces Better CIL Performance

The key theoretical result in Section 3 is that better OOD detection will produce better CIL performance. We compare a weaker OOD method ODIN with the strong CSI. ODIN is a post-processing method for OOD detection [36]. Note that it does not always improves the OOD detection performance compared to without the ODIN post-processing (see below).

---

<sup>4</sup>The Sup paper proposed an one-shot task-id prediction assuming that the test instances come in a batch and all belong to the same task like iTAML. We assume a single test instance per batch. Its task-id prediction results in accuracy of 50.2 on C10-5T, which is much lower than 62.6 by using Eq. 21. The task-id prediction of HyperNet also works poorly. The accuracy by its task-id prediction is 49.34 on C10-5T while it is 53.4 using Eq. 21. PR uses entropy to find task-id. Among many variations of PR, we use the variations that perform the best for each dataset with exemplar-free and single sample per batch at testing (i.e., no PR-BW).

Table 1: Performance Comparison between the Original Output and ODIN

Method	AUC		CIL	
	Original	ODIN	Original	ODIN
OWM	71.31	70.06	28.91	28.88
MUC	72.69	72.53	30.42	29.79
PASS	69.89	69.60	33.00	31.00
LwF	88.30	87.11	45.26	51.82
A-GEM	78.01	79.00	9.29	13.48
EEIL	83.37	79.73	48.99	41.74
GD	85.37	82.98	49.67	47.28
BiC	87.89	86.73	52.92	48.65
DER++	85.99	88.21	53.71	55.29
HAL	64.21	64.83	15.59	21.01
HAT	77.72	77.80	41.06	41.21
HyperNet	71.82	72.32	30.23	30.83
Sup	79.16	80.58	44.58	46.74

Performance comparison based on C100-10T between the original output and the output post-processed with OOD detection technique ODIN. Note that ODIN is not applicable to iCaRL and Mnemonics as they are not based on softmax but some distance functions. As mentioned earlier, for **Co<sup>2</sup>L**, **CCG**, and **PR-Ent**, they either have no code or their codes do not run on our machine. The results for other datasets are in Appendix B.

**Applying ODIN.** We first train the baseline models using their original algorithms, and then apply temperature scaling and input noise of ODIN at testing for each task (no training data needed). More precisely, the output of class  $j$  in task  $k$  changes by temperature scaling factor  $\tau_k$  of task  $k$  as

$$s(x; \tau_k)_j = e^{f(x)_{kj}/\tau_k} / \sum_j e^{f(x)_{kj}/\tau_k} \quad (22)$$

and the input changes by the noise factor  $\epsilon_k$  as

$$\tilde{x} = x - \epsilon_k \text{sign}(-\nabla_x \log s(x; \tau_k)_{\hat{y}}) \quad (23)$$

where  $\hat{y}$  is the class with the maximum output value in task  $k$ . This is a positive adversarial example inspired by [16]. The values  $\tau_k$  and  $\epsilon_k$  are hyper-parameters and we use the same values for all tasks except for PASS, for which we use a validation set to tune  $\tau_k$  (see Appendix B).

Table 1 gives the results for C100-10T. The CIL results clearly show that the CIL performance increases if the AUC increases with ODIN. For instance,

Table 2: Average CIL and AUC after Applying OOD Detection Methods ODIN and CSI

CL	OOD	C10-5T		C100-10T		C100-20T		T-5T		T-10T	
		AUC	CIL	AUC	CIL	AUC	CIL	AUC	CIL	AUC	CIL
HAT	ODIN	82.5	62.6	77.8	41.2	75.4	25.8	72.3	38.6	71.8	30.0
	CSI	91.2	87.8	84.5	63.3	86.5	54.6	76.5	45.7	78.5	47.1
Sup	ODIN	82.4	62.6	80.6	46.7	81.6	36.4	74.0	41.1	74.6	36.5
	CSI	91.6	86.0	86.8	65.1	88.3	60.2	77.1	48.9	79.4	45.7

Average CIL and AUC of HAT and Sup with OOD detection methods ODIN and CSI. ODIN is a traditional OOD detection method while CSI is a recent OOD detection method known to be better than ODIN. As CL methods produce better OOD detection performance by CSI, their CIL performances are better than the ODIN counterparts.

the CIL of DER++ and Sup improves from 53.71 to 55.29 and 44.58 to 46.74, respectively, as the AUC increases from 85.99 to 88.21 and 79.16 to 80.58. It shows that when this method is incorporated into each task model in existing trained CIL network, the CIL performance of the original method improves. We note that ODIN does not always improve the average AUC. For those experienced a decrease in AUC, the CIL performance also decreases except LwF. The inconsistency of LwF is due to its severe classification bias towards later tasks as discussed in BiC [62]. The temperature scaling in ODIN has a similar effect as the bias correction in BiC, and the CIL of LwF becomes close to that of BiC after the correction. Regardless of whether ODIN improves AUC or not, the positive correlation between AUC and CIL (except LwF) verifies the efficacy of Theorem 3, indicating better OOD detection results in better CIL performances.

**Applying CSI.** We now apply the OOD detection method CSI. Due to its sophisticated data augmentation, supervised constrative learning and results ensemble, it is hard to apply CSI to other baselines without fundamentally change them except for HAT and Sup (SupSup) as these methods are parameter isolation-based TIL methods. We can simply replace their model for training each task with CSI wholesale. As mentioned earlier, both HAT and Sup as TIL methods have almost no forgetting.

Table 2 reports the results of using CSI and ODIN. ODIN is a weaker OOD method than CSI. Both HAT and Sup improve greatly as the systems are equipped with a better OOD detection method CSI. These experiment results empirically demonstrate the efficacy of Theorem 3, i.e., the CIL performance can be improved if a better OOD detection method is used.

Table 3: Average Accuracy (CIL) of All Methods

	Method	C10-5T	C100-10T	C100-20T	T-5T	T-10T	Avg.
(a)	<i>OWM</i>	51.8±0.05	28.9±0.60	24.1±0.26	10.0±0.55	8.6±0.42	24.7
(b)	<i>MUC</i>	52.9±1.03	30.4±1.18	14.2±0.30	33.6±0.19	17.4±0.17	29.7
	<i>PASS</i> <sup>†</sup>	47.3±0.98	33.0±0.58	25.0±0.69	28.4±0.51	19.1±0.46	30.6
(c)	LwF	54.7±1.18	45.3±0.75	44.3±0.46	32.2±0.50	24.3±0.26	40.2
	iCaRL*	63.4±1.11	51.4±0.99	47.8±0.48	37.0±0.41	28.3±0.18	45.6
	A-GEM	20.0±0.37	9.3±0.17	4.1±0.89	13.5±0.08	7.7±0.07	10.9
	EEIL	57.1±0.28	49.0±1.27	33.5±0.08	14.7±0.40	9.8±0.19	32.8
	GD	58.7±0.31	49.7±0.33	38.9±0.02	16.4±1.40	11.7±0.25	35.1
	Mnemonics <sup>†*</sup>	64.1±1.47	51.0±0.34	47.6±0.74	37.1±0.46	28.5±0.72	45.7
	BiC	61.4±1.74	52.9±0.64	48.9±0.54	41.7±0.74	33.8±0.40	47.7
	DER++	66.0±1.20	53.7±1.30	46.6±1.44	35.8±0.77	30.5±0.47	46.5
	HAL	32.8±2.17	15.6±0.31	13.5±1.53	3.4±0.35	3.4±0.38	13.7
	Co <sup>2</sup> L	65.6					
	<i>CCG</i>	70.1					
(d)	<i>HAT</i>	62.7±1.45	41.1±0.93	25.6±0.51	38.5±1.85	29.8±0.65	39.5
	<i>HyperNet</i>	53.4±2.19	30.2±1.54	18.7±1.10	7.9±0.69	5.3±0.50	23.1
	<i>Sup</i>	62.4±1.45	44.6±0.44	34.7±0.30	41.8±1.50	36.5±0.36	44.0
	<i>PR-Ent</i>	61.9	45.2				
(e)	<i>HAT+CSI</i>	87.8±0.71	63.3±1.00	54.6±0.92	45.7±0.26	47.1±0.18	59.7
	<i>Sup+CSI</i>	86.0±0.41	65.1±0.39	60.2±0.51	48.9±0.25	45.7±0.76	61.2
	HAT+CSI+c	88.0±0.48	65.2±0.71	58.0±0.45	51.7±0.37	47.6±0.32	62.1
	Sup+CSI+c	87.3±0.37	65.2±0.37	60.5±0.64	49.2±0.28	46.2±0.53	61.7

Average accuracy after all tasks are learned. The baselines are grouped into (a), (b), (c), and (d) for projection, regularization, replay, and parameter-isolation methods, respectively. Our proposed methods are grouped into (e). Exemplar-free methods are italicized. † indicates that in their original papers, PASS and Mnemonics are pre-trained with the first half of the classes. Their results with pre-train are 50.1 and 53.5 on C100-10T, respectively, which are still much lower than the proposed HAT+CSI and Sup+CSI without pre-training. We do not use pre-training in our experiment for fairness. \* indicates that iCaRL and Mnemonics report average incremental accuracy in their original papers. We report average accuracy over all classes after all tasks are learned. The last column Avg. shows the average CIL accuracy of each method over all datasets.

#### 4.2.4. Full Comparison of HAT+CSI and Sup+CSI with Baselines

We now make a full comparison of the two proposed systems HAT+CSI and Sup+CSI designed based on the theoretical results with baselines. Since HAT and Sup are exemplar-free CL methods, HAT+CSI and Sup+CSI do not need to save any previous task data for replaying. Table 3 shows that HAT and Sup equipped with CSI outperform the baselines by large margins. DER++, the best replay method, achieves 66.0 and 53.7 on C10-5T and C100-10T, respectively, while HAT+CSI achieves 87.8 and 63.3 and Sup+CSI achieves 86.0 and 65.1. The large performance gap remains consistent in more challenging problems, T-5T and T-10T.



Table 4: TIL Accuracy

Method	C10-5T	C100-10T	C100-20T	T-5T	T-10T	Avg.
BiC	95.4±0.35	84.6±0.48	88.7±0.19	61.5±0.60	62.2±0.45	78.5
HAT	96.7±0.18	84.0±0.23	85.0±0.98	61.2±0.72	63.8±0.41	78.1
Sup	96.6±0.21	87.9±0.27	91.6±0.15	64.3±0.24	68.4±0.22	81.8
HAT+CSI	98.7±0.06	92.0±0.37	94.3±0.06	68.4±0.16	72.4±0.21	85.2
Sup+CSI	98.7±0.07	93.0±0.13	95.3±0.20	65.9±0.25	74.1±0.28	85.4

TIL (WP) results of 3 best performing baselines and our methods. The full results are given in Appendix E. The calibrated versions (+c) of our methods are omitted as calibration does not affect TIL performances.

Due to the definition of OOD in the prediction method and the fact that each task is trained separately in HAT and Sup, the outputs  $f(x)_k$  from different tasks can be in different scales, which will result in incorrect predictions. To deal with the problem, we can calibrate the output as  $\alpha_k f(x)_k + \beta_k$  and use  $OOD_k = \sigma(\alpha_k f(x)_k + \beta_k)$ . The optimal  $\alpha_k^*$  and  $\beta_k^*$  for each task  $k$  can be found by optimization with a memory buffer to save a very small number of training examples from previous tasks like that in the replay-based methods. We refer the calibrated methods as HAT+CSI+c and Sup+CSI+c. They are trained by using the memory buffer of the same size as the replay methods (see Section 4.2.2). Table 3 shows that the calibration improves from their memory free versions, i.e., without calibration. We provide the details about how to train the calibration parameters  $\alpha_k$  and  $\beta_k$  in Appendix D.

As shown in Theorem 1, the CIL performance also depends on the TIL (WP) performance. We compare the TIL accuracies of the baselines and our methods in Table 4. Our systems again outperform the baselines by large margins on more challenging datasets (e.g., CIFAR100 and Tiny-ImageNet).

## 5. Proposed Approach 2: Out-of-Distribution Replay

The approach presented above does not save any training data from previous tasks except for the optional step of calibration. The method presented in this section is based on the replay approach to solving CIL, which saves a small number of training data from each previous task. The proposed method is called *Multi-head model for continual learning via OOD REplay (MORE)*.

### 5.1. The Proposed MORE Technique

Recall a replay-based method for continual learning works by memorizing or saving a small subset of the training samples from each previous task in a memory buffer. The saved data is called the *replay data*. In learning a new task, the new task data and the replay data are trained jointly to update the model. Clearly, using the replay data can partially deal with the inter-class separation (ICS) problem because the model sees some data from all classes learned so far. However, it cannot solve the ICS problem completely because the amount of the replay data is often very small.

Unlike existing replay-based CIL methods, which simply use the replay data to update the decision boundaries between the old class and the new classes (in the new task), the proposed method uses the replay data to build an OOD detection model for each task in continual learning, which gives the name of the proposed method, i.e., *out-of-distribution replay*. Further, unlike existing OOD detection methods, which usually do not use any OOD data in training, the proposed method uses the replay data from previous tasks as the OOD data for the current new task in building its OOD detection model.

Unlike HAT+CSI and Sup+CSI, which do not use a pre-trained network, MORE trains a multi-head network as an adapter [23] to a pre-trained network (see Figure 2(b)). Note that using a pre-trained transformer network and adapter modules is a common practice in existing continual learning methods in the natural language processing community [26]. Here we also leverage this approach for image classification tasks. In continual learning, the pre-trained network is frozen, only the adapters and the norm layers are trainable. Similar to HAT+CSI, hard attention mask (HAT) is again employed to protect each task model or classifier to avoid forgetting. Each head is also an OOD detection model for a task, but, as mentioned above, MORE uses the replay data as the OOD data to build an OOD detection model. Since HAT has been described in Section 4.1.1, we will not discuss it further except to state that we need to use  $\mathcal{L}_{ood}$  in Eq. 24 to replace  $\mathcal{L}_{ce}$  in Eq. 13 after incorporating the trainable embedding  $e^k$ . We describe the whole training and prediction process in Appendix H.

#### 5.1.1. Training an OOD Detection Model

At task  $k$ , the system receives the training data  $\mathcal{D}_k = \{(x_k^i, y_k^i)_{i=1}^{n_k}\}$ , where  $n_k$  is the number of samples, and  $x_k^i \in \mathbf{X}_k$  is an input sample and  $y_k^i \in \mathbf{Y}_k$  (the set of all classes of task  $k$ ) is its class label. We train the feature extractor  $z = h(x, k; \theta)$  and task specific classifier  $f(z; \phi_k)$  using  $\mathcal{D}_k$  and the samples in

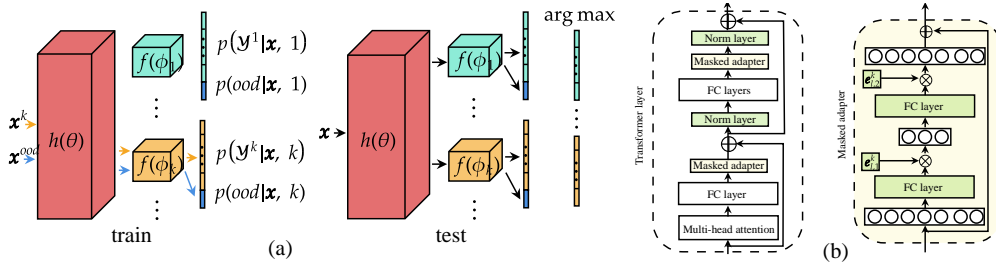


Figure 2: (a) We train the feature extractor and the task classifier  $k$  at task  $k$ . The output values of the classifier correspond to  $|\mathbf{Y}_k| + 1$  classes, in which the last class is for OOD (i.e., representing previous and unseen future classes). At inference/testing, the probability values of each task model without the OOD class are concatenated and the system chooses the class with the maximum score. (b) Transformer and adapter module. The masked adapter network consists of 2 fully connected layers and task specific masks. During training, only the masked adapters and norm layers are updated and the other parts in the transformer layers remain unchanged.

the memory buffer  $\mathcal{M}$ . We treat the buffer data as OOD data to encourage the network to learn the current task and also detect OOD samples (the models or classifiers of the previous tasks are not touched). We achieve it by maximizing  $p(y|x, k) = \text{softmax}f(h(x, k; \theta); \phi_k)$  for an IND sample  $x \in \mathbf{X}_k$  and maximizing  $p(ood|x, k)$  for an OOD sample  $x \in \mathcal{M}$ . The additional label *ood* is reserved for previous and possible future unseen classes. Figure 2(a) shows the overall idea of the proposed approach. We formulate the problem as follows.

Given the training data  $\mathbf{X}_k$  of size  $n_k$  at task  $k$  and the memory buffer  $\mathcal{M}$  of size  $M$ , we minimize the loss

$$\mathcal{L}_{ood}(\theta, \phi_k) = -\frac{1}{M + N} \left( \sum_{(x,y) \in \mathcal{M}} \log p(ood|x, k) + \sum_{(x,y) \in \mathcal{D}^k} \log p(y|x, k) \right) \quad (24)$$

It is the sum of two cross-entropy losses. The first loss is for learning OOD samples while the second loss is for learning the classes from the current task. We optimize the shared parameter  $\theta$  in the feature extractor. The task specific classification parameters  $\phi_k$  are independent of other tasks. The learned representation on the current data should be robust to OOD data. The classifier thus can classify both IND and OOD data.

In testing, we perform prediction by comparing the softmax probability output values using all the task classifiers from task 1 to  $k$  without the OOD

class as

$$\hat{y} = \arg \max \bigoplus_{1 \leq j \leq k} p(\mathbf{Y}_j|x, j) \quad (25)$$

where  $\bigoplus$  is the concatenation over the output space. Figure 2(a) shows the prediction rule. We are basically choosing the class with the highest softmax probability over all classes from all learned tasks.

### 5.1.2. Back-Updating the Previous OOD Models

Each task model works better if more diverse OOD data is provided during training. As in a replay-based approach, MORE saves an equal number of samples per class after each task [12]. The saved samples in the memory are used as OOD samples for each new task. Thus, in the beginning of continual learning when the system is trained on only a small number of tasks, the classes of samples in the memory are less diverse than after more tasks are learned. This makes the performance of OOD detection stronger for later tasks, but weaker in earlier tasks. To prevent this asymmetry, we update the model of each previous task so that it can also identify the samples from subsequent classes (which were unseen during the training of the previous task) as OOD samples.

At task  $k$ , we update the previous task models ( $j = 1, \dots, k - 1$ ) as follows. Denote the samples of task  $j$  in memory  $\mathcal{M}$  by  $\tilde{\mathbf{X}}_j$ . We construct a new dataset using the current task dataset and the samples in the memory buffer. We randomly select  $|\mathcal{M}|$  samples from the training data  $\mathcal{D}_k$  and pool them with the remaining samples in  $\mathcal{M}$  after removing the IND samples  $\tilde{\mathcal{D}}_j$  of task  $j$  from  $\mathcal{M}$ . We do not use the entire training data  $\mathcal{D}_k$  as we do not want a large sample imbalance between IND and OOD. Denote the new dataset by  $\tilde{\mathcal{M}}$ . Using the data, we update only the parameters  $\phi_j$  of the classifier for task  $j$  with the feature representations frozen by minimizing the loss

$$\mathcal{L}(\phi_j) = -\frac{1}{2M} \left( \sum_{(x,y) \in \tilde{\mathcal{M}}} \log p(\text{ood}|x, j) + \sum_{(x,y) \in \tilde{\mathcal{D}}_j} \log p(y|x, j) \right) \quad (26)$$

We reduce the loss by updating the parameters of classifier  $j$  to maximize the probability of the class if the sample belongs to task  $j$  and maximize the OOD probability otherwise.

### 5.1.3. Improving Prediction Performance by a Distance Based Technique

We further improve the prediction in Eq. 25 by introducing a distance based factor used as a coefficient to the softmax probabilities in Eq. 25. It is quite intuitive that if a test instance is close to a class, it is more likely to belong to the class. We thus propose to combine this new distance factor and the softmax probability output of the task  $j$  model to make the final prediction decision. In some sense, this can be considered as an ensemble of the two methods.

We define the distance based coefficient  $s_j(x)$  of task  $j$  for the test instance  $x$  by the maximum of inverse Mahalanobis distance [33] between the feature of  $x$  and the Gaussian distributions of the classes in task  $j$  parameterized by the mean  $\mu_j^i$  of the class  $i$  in task  $j$  and the sample covariance  $S_j$ . They are estimated by the features of class  $i$ 's training data for each class  $i$  in task  $j$ . If a test instance is from the task, its feature should be close to the distribution that the instance belongs to. Conversely, if the instance is OOD to the task, its feature should not be close to any of the distributions of the classes in the task. More precisely, for task  $j$  with class  $y_1, \dots, y_{|\mathbf{Y}_j|}$  (where  $|\mathbf{Y}_j|$  represents the number of classes in task  $k$ ), we define the coefficient  $s_j(x)$  as

$$s_j(x) = \max \left[ 1/\text{MD}(x; \mu_j^{y_1}, S_j), \dots, 1/\text{MD}(x; \mu_j^{y_{|\mathbf{Y}_j|}}, S_j) \right] \quad (27)$$

$\text{MD}(x; \mu_j^i, S_j)$  is the Mahalanobis distance. The coefficient is large if at least one of the Mahalanobis distances is small but the coefficient is small if all the distances are large (i.e. the feature is far from all the distributions of the task). The parameters  $\mu_j^i$  and  $S_j$  can be computed and saved when each task is learned. The mean  $\mu_j^i$  is computed using the training samples  $\mathcal{D}_j^i$  of class  $i$  as follows,

$$\mu_j^i = \sum_{x \in \mathcal{D}_j^i} h(x, i) / |\mathcal{D}_j^i| \quad (28)$$

and the covariance  $S_j$  of task  $j$  is the mean of covariances of the classes in task  $j$ ,

$$S_j = \sum_{i \in \mathbf{Y}_j} S_j^i / |\mathbf{Y}_j| \quad (29)$$

where  $S_j^i = \sum_{x \in \mathcal{D}_j^i} (x - \mu_j^i)^T (x - \mu_j^i) / |\mathcal{D}_j^i|$  is the sample covariance of class  $i$ . By multiplying the coefficient  $s_j(x)$  to the original softmax probabilities

$p(\mathbf{Y}_j|x, j)$ , the task output  $p(\mathbf{Y}_j|x, j)s_j(x)$  increases if  $x$  is from task  $j$  and decreases otherwise. The final prediction is made by (which replaces Eq. 25)

$$y = \arg \max_{1 \leq j \leq k} \bigoplus p(\mathbf{Y}_j|x, j)s_j(x), \quad (30)$$

where  $k$  is the last task that we have learned.

## 5.2. Experiments

We now report the experiment results of the proposed method MORE. For **experimental datasets**, we use the same three image classification benchmark datasets as in Section 4.2.1. For **baselines**, the same systems are used as well (see Section 4.2.1) except Mnemonics, HyperNet, CCG, Co<sup>2</sup>L, and PR-Ent. Mnemonics requires optimization of training instances and it is not clear how to implement for images after interpolation for a given input size of a pre-trained model (see below). For HyperNet, it is due to the reason explained in Training Details in Section 4.2.2. For CCG, Co<sup>2</sup>L, and PR-Ent, CCG has no code and the codes of Co<sup>2</sup>L, and PR-Ent do not run in our environment and thus we could not convert their codes to use a pre-trained model. Finally, we are left with 13 baselines. Note that HAT-CSI and Sup+CSI are not included as they are much weaker (up to 15% lower than MORE in accuracy) as CSI’s approach of using contrastive learning and data augmentations does not work well with a pre-trained model.

**Evaluation Metrics.** We still use the same evaluation measures as we used in Section 4.2.2. **(1).** *Average classification accuracy* over all classes after learning the last task. **(2).** *Average AUC* (Area Under the ROC Curve) for evaluating OOD detection performance of continual learning in the open world. See Section 5.2.4 for more details.

### 5.2.1. Pre-trained Network

We pre-train a vision transformer [59] using a subset of the ImageNet data [52] and apply the pre-trained network/model to all baselines and our method. To ensure that there is no overlapping of data between ImageNet and our experimental datasets, we manually removed 389 classes from the original 1000 classes in ImageNet that are similar/identical to the classes in CIFAR-10, CIFAR-100, or Tiny-ImageNet. We pre-train the network with the remaining subset of 611 classes of ImageNet.

Using the pre-trained network, both our system and the baselines improve dramatically compared to their versions without using the pre-trained

network. For instance, the two best baselines (DER++ and PASS) in our experiments achieve the average classification accuracy of 66.89 and 68.25 (after the final task) with the pre-trained network over 5 experiments while they achieve only 46.88 and 32.42 without using the pre-train network.

We insert an adapter module at each transformer layer to exploit the pre-trained transformer network in continual learning. During training, the adapter module and the layer norm are trained while the transformer parameters are unchanged to prevent forgetting in the pre-trained network.

### 5.2.2. Training Details

For all experiments, we use the same backbone architecture DeiT-S/16 [59] with a 2-layer adapter [23] at each transformer layer, and the same class order for both baselines and our method. The first fully-connected layer in adapter maps from dimension 384 to bottleneck. The second fully-connected layer following ReLU activation function maps from bottleneck to 384. The the bottleneck dimension is the same for all adapters in a model. For our method, we use SGD with momentum value 0.9. The back-updating method in Section 5.1.2 is also a hyper-parameter choice. If we apply it, we train each classifier for 10 epochs by SGD with learning rate 0.01, batch size 16, and momentum value 0.9. We choose 500 for  $s$  in Eq. 8 and 0.75 for  $\lambda$  in Eq. 12 as recommended in [55]. We find a good set of learning rate and number of epochs on the validation set made of 10% of the training data. We follow [12] and save an equal number of random samples per class in the replay memory. Following the experiment settings in [51, 69], we fix the size of memory buffer and reduce the saved samples to accommodate a new set of samples after a new task is learned. We use the class order protocol in [51, 7] by generating random class orders for the experiments. The baselines and our method use the same class ordering. We also report the size of memory required for each experiment in Appendix I.

For CIFAR-10, we split 10 classes into 5 tasks (2 classes per task). The bottleneck size in each adapter is 64. Following [7], we use the memory size 200, and train for 20 epochs with learning rate 0.005, and apply the back-updating method in Section 5.1.2.

For CIFAR-100, we conduct 10 tasks and 20 tasks experiments, where each task has 10 classes and 5 classes, respectively. We double the bottleneck size of the adapter to learn more classes. We use the memory size 2000 following [51] and train for 40 epochs with learning rate 0.001 and 0.005 for 10 tasks and 20 tasks, respectively, and apply the back-updating method in

Table 5: Average Accuracy after the Final Task

	Method	C10-5T	C100-10T	C100-20T	T-5T	T-10T	Avg.
(a)	OWM	41.69±6.34	21.39±3.18	16.98±4.44	24.55±2.48	17.52±3.45	24.43
(b)	MUC	73.95±7.24	57.87±1.11	43.98±2.68	62.47±0.34	55.79±0.49	58.81
	PASS	86.21±1.10	68.90±0.94	66.77±1.18	61.03±0.38	58.34±0.42	68.25
(c)	LwF	67.59±4.27	66.50±1.93	67.54±0.97	33.51±4.36	36.85±4.46	54.40
	iCaRL	87.55±0.99	68.90±0.47	69.15±0.99	53.13±1.04	51.88±2.36	66.12
	A-GEM	56.33±7.77	25.21±4.00	21.99±4.01	30.53±3.99	21.90±5.52	31.20
	EEIL	82.34±3.13	68.08±0.51	63.79±0.66	53.34±0.54	50.38±0.97	63.59
	GD	<b>89.16±0.53</b>	64.36±0.57	60.10±0.74	53.01±0.97	42.48±2.53	61.82
	BiC	67.44±3.93	64.47±1.30	67.69±1.97	38.78±1.26	40.98±2.39	55.87
	DER++	84.63±2.91	69.73±0.99	70.03±1.46	55.84±2.21	54.20±3.28	66.89
	HAL	84.38±2.70	67.17±1.50	67.37±1.45	52.80±2.37	55.25±3.60	65.39
(d)	HAT	83.30±1.54	62.34±0.93	56.72±0.44	57.91±0.72	53.12±0.94	62.68
	Sup	80.91±2.99	62.49±0.49	57.32±1.11	58.43±0.67	54.52±0.45	62.74
	MORE	<b>89.16±0.96</b>	<b>70.23±2.27</b>	<b>70.53±1.09</b>	<b>64.97±1.28</b>	<b>63.06±1.26</b>	<b>71.59</b>

Average accuracy after the final task. ‘-XT’ means X number of tasks. Our system MORE and all baselines used the pre-trained network. The baselines are grouped into (a), (b), (c), and (d) for projection, regularization, replay, and parameter-isolation methods, respectively. The last column show the average accuracy of each method over all datasets and experiments. We highlight the best results in each column in bold.

### Section 5.1.2.

For Tiny-ImageNet, two experiments are conducted. We split 200 classes into 5 and 10 tasks, where each task has 40 classes and 20 classes per task, respectively. We use the bottleneck size 128, and save 2000 samples in memory. We train with learning rate 0.005 for 15 and 10 epochs for 5 tasks and 10 tasks, respectively. There is no need to use the back-updating method as the earlier tasks already have diverse OOD classes.

### 5.2.3. Accuracy and Forgetting Rate Results and Analysis

**Average Accuracy.** Table 5 shows that our method MORE consistently outperforms the baselines. All the reported results are the averages of 5 runs. The last column gives the average of each row. We compare with the replay-based methods first. The best replay-based method on average over all the datasets is DER++. Our method MORE achieves the accuracy of 71.59, much better than 66.89 of DER++. This demonstrates that the existing replay-based methods utilizing the replay samples to update all learned classes are inferior to our MORE method using samples for OOD learning. The best baseline is the generative method PASS. Its average accuracy over



Table 6: Average Accuracy with Smaller Memory Sizes

	Method	C10-5T	C100-10T	C100-20T	T-5T	T-10T	Avg.
(a)	OWM	41.69±6.34	21.39±3.18	16.98±4.44	24.55±2.48	17.52±3.45	24.43
(b)	MUC	73.95±7.24	57.87±1.11	43.98±2.68	62.47±0.34	55.79±0.49	58.81
	PASS	86.21±1.10	68.90±0.94	66.77±1.18	61.03±0.38	58.34±0.42	68.25
(c)	LwF	63.01±4.19	56.76±3.72	63.53±2.86	26.79±2.36	28.08±4.88	47.63
	iCaRL	86.08±1.19	66.96±2.08	68.16±0.71	47.27±3.22	49.51±1.87	63.60
	A-GEM	56.64±4.29	23.18±2.54	20.76±2.88	31.44±3.84	23.73±6.27	31.15
	EEIL	77.44±3.04	62.95±0.68	57.86±0.74	48.36±1.38	44.59±1.72	58.24
	GD	85.96±1.64	57.17±1.06	50.30±0.58	46.09±1.77	32.41±2.75	54.39
	BiC	56.28±3.31	58.42±2.48	62.19±1.20	33.29±2.65	28.44±2.41	47.72
	DER++	80.09±3.00	64.89±2.48	65.84±1.46	50.74±2.41	49.24±5.01	62.16
	HAL	79.16±4.56	62.65±0.83	63.96±1.49	48.17±2.94	47.11±6.00	60.21
(d)	HAT	83.30±1.54	62.34±0.93	56.72±0.44	57.91±0.72	53.12±0.94	62.68
	Sup	80.91±2.99	62.49±0.49	57.32±1.11	58.43±0.67	54.52±0.45	62.74
	MORE	<b>88.13±1.16</b>	<b>71.69±0.11</b>	<b>71.29±0.55</b>	<b>64.17±0.77</b>	<b>61.90±0.90</b>	<b>71.44</b>

Accuracy performances of the baselines and our method MORE with smaller memory sizes. We reduce the size of the memory buffer by half. The new sizes are 100, 1000, 1000 for CIFAR10, CIFAR100, and Tiny-ImageNet. Numbers in bold are the best results in each column.

all the datasets is 68.25, which is still poorer than our method’s performance of 71.59. The performance of the multi-head method HAT [55] using task-id prediction is only 62.68, which is lower than many other baselines. Its performance is particularly low in experiments where the number of classes per task is small. For instance, its accuracy on C100-20T is 56.72, much lower than our method of 70.53 trained based on OOD detection.

**Accuracy with Smaller Memory Sizes.** For all the datasets, we run additional experiments with half of the original memory size and show that our method is even stronger with a smaller memory. The new memory sizes are 100, 1000, and 1000 for CIFAR-10, CIFAR-100, and Tiny-ImageNet, respectively. Table 6 shows that MORE has experienced almost no performance drop with the reduced memory size while the memory-based baselines suffer from major performance reduction. The accuracy of the best memory-based baseline (DER++) has decreased the accuracy from 66.89 to 62.16, while MORE only decreases from 71.59 to 71.44, which shows that a small number of OOD samples is enough to enable the system to produce a robust OOD detection model.

**Average Forgetting Rate.** The average forgetting rate is defined as

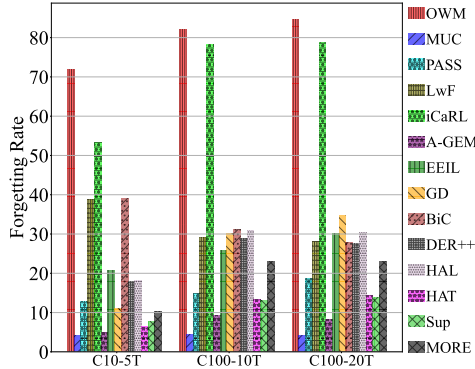


Figure 3: Average forgetting rate (%). The lower the rate, the better the method is.

follows [40]:  $\mathcal{F}^t = \sum_{k=1}^{t-1} (\mathcal{A}_k^{\text{init}} - \mathcal{A}_k^t) / (t - 1)$ , where  $\mathcal{A}_k^{\text{init}}$  is the classification accuracy on samples of task  $k$  right after learning the task  $k$ . We do not consider the task  $t$  as it is the last task.

We compare the forgetting rate of our method MORE against the baselines using C10-5T, C100-10T, and C100-20T. Figure 3 shows that the performance drop of our method as more task are learned is relatively lower than many baselines. MUC, A-GEM, HAT, and Sup achieve lower drop than our method. However, they are not able to adapt to new tasks well as the accuracy values of the four methods on C100-10T are 57.87, 25.21, 62.34, and 62.49, respectively, while our method MORE achieves 70.23. The performance gaps remains consistent in the other dataset. PASS experiences smaller drop in performance on C100-10T and C100-20T than our method, but its accuracy of 68.90 and 66.77 are significantly lower than 70.23 and 70.53 of our MORE.

#### 5.2.4. Out-of-Distribution Detection Results

As we explained in the introduction section, since our method MORE is based on OOD detection in building each task model, our method can naturally be used to detect test samples that are out-of-distribution for all the classes or tasks learned thus far. We are not aware of any existing continual learning system that has done such an evaluation. We evaluate the performance of the baselines and our system in this out-of-distribution scenario, which is also called the open set setting.

This OOD detection ability is highly desirable for a continual learning system because in a real-life environment in the open world, the system can

Table 7: AI-AUC Results

	Method	C10-5T	C100-10T	C100-20T	T-5T	T-10T	Avg.
(a)	OWM	70.02±3.59	63.17±1.06	59.42±1.26	67.24±0.92	62.17±0.35	64.41
(b)	MUC	85.47±3.97	79.28±1.15	74.82±1.91	<b>83.91±0.54</b>	<b>81.42±0.47</b>	80.98
	PASS	84.57±1.54	77.74±1.40	77.42±1.44	77.07±2.14	74.79±2.36	78.32
(c)	LwF	72.18±4.15	74.95±0.39	75.40±0.64	66.44±1.14	65.52±0.64	70.90
	iCaRL	82.12±5.38	77.42±0.45	76.91±1.30	71.86±1.57	74.24±1.66	76.06
	A-GEM	74.92±5.62	64.19±0.86	60.23±0.95	67.88±1.28	63.08±1.12	66.06
	EEIL	87.19±2.31	78.89±1.32	77.69±1.40	74.82±0.79	73.45±1.33	78.39
	GD	<b>89.71±1.85</b>	77.31±1.03	75.19±0.87	75.36±0.78	70.90±1.75	77.69
	BiC	71.29±3.57	74.49±0.72	75.71±0.60	67.45±0.89	66.63±0.77	71.11
	DER++	84.61±2.64	78.42±0.64	78.37±0.42	74.80±1.72	74.86±1.93	78.09
	HAL	84.09±3.30	77.37±0.55	77.66±0.31	74.52±1.93	75.47±2.35	77.82
(d)	HAT	87.83±2.44	79.57±0.29	77.20±0.74	79.78±1.59	78.25±1.68	80.53
	Sup	87.06±3.68	80.54±0.12	77.81±0.66	80.01±0.71	78.96±0.64	80.87
	MORE	88.06±1.84	<b>81.67±1.27</b>	<b>80.97±0.80</b>	80.72±3.38	79.73±2.97	<b>82.23</b>

Numbers in bold are the best results in each column.

be exposed to not only seen classes, but also unseen classes. When the test sample is from one of seen classes, the system should be able to predict its class. If the sample does not belong to any of the training classes seen so far (i.e., the sample is out-of-distribution), the system should detect it.

We formulate the performance of OOD detection of a continual learning system as the following. A continual learning system accepts and classifies a test sample after training task  $k$  if the test sample is from one of the classes in tasks  $1, \dots, k$ . If it is from one of the classes of the future tasks  $k + 1, \dots, t$ , it should be rejected as OOD (where  $t$  is the last task in each evaluation).

We use maximum softmax probability (MSP) [20] as the OOD score of a test sample for the baselines and use maximum output with coefficient in Eq. 30 for our method MORE. We employ Area Under the ROC Curve (AUC) to measure the performance of OOD detection as AUC is the standard metric used in OOD detection papers [65]. We report *average incremental AUC* (AI-AUC) which is the average AUC result at all tasks except the last one as there is no more OOD data after the last task.

Table 7 shows that our method MORE outperforms all baselines consistently except MUC and GD. For MUC, it performs better than MORE on Tiny-ImageNet, but on average, it is poorer (80.98) than MORE (82.23). For GD, it outperforms MORE on C10-5T, but its overall performance is much lower as it achieves the average of only 77.69 over the 5 experiments.

Table 8: Ablation Study

	C10-5T	C100-10T	C100-20T
Original	91.01±2.48	76.93±1.58	75.76±2.35
Coefficient (C)	93.86±1.12	80.31±1.02	80.77±1.36
Back (B)	93.36±0.79	80.35±1.08	80.32±0.82
C + B	94.23±0.82	81.24±1.24	81.59±0.98

Performance gains with the proposed techniques. The row Original indicates the method without the coefficient and back-updating and the row Back means the back-updating method.

### 5.2.5. Ablation Study

We conduct an ablation study to measure the performance gain by each proposed technique, **back-updating** in previous models in Section 5.1.2 and the **distance-based coefficient** in Section 5.1.3, using three experiments. The back-updating by Eq. 26 is to improve the earlier task models as they are trained with less diverse OOD data than later models. The modified output with coefficient in Eq. 27 is to improve the classification accuracy by combining the softmax probability of the task networks and the inverse Mahalanobis distances.

Table 8 compares accuracy obtained after applying each method. Both distance based coefficient and back-updating show large improvements from the original method without any of the two techniques. Although the performance is already competitive with either technique, the performance improves further after applying them together.

## 6. Conclusion

This paper studied open world continual learning, which is necessary for learning in the open world. An open world learning algorithm first needs to detect novel or out-of-distribution (OOD) items and then learn them continually or incrementally. This type of learning is called class incremental learning (CIL), which is a challenging setting of continual learning. Another popular setting is task incremental learning (TIL). Traditionally, novelty/OOD detection and CIL are regarded as two completely different problems. This paper theoretically showed that the two problems can be unified. In particular, we first decomposed the CIL prediction problem into *within-task prediction* (WP) and *task-id prediction* (TP). WP is basically TIL. The

paper further theoretically demonstrated that TP is correlated with *out-of-distribution* (OOD) detection. It then proved that a good performance of the two is both necessary and sufficient for good CIL performances. Since OOD detection is basically novelty detection in open-world learning, our theory connects and unifies open-world novelty detection and continual learning (CIL in particular). Their combination gives us the paradigm of open-world continual learning. The theoretical result also provides a principled guidance for designing better continual learning algorithms. Based on the result, several new CIL methods have been designed. They outperform strong baselines in CIL by a large margin and also perform novelty (or OOD) detection well in the open world continual learning setting.

### **Author Contributions**

Gyuhak Kim conceived the idea, developed the algorithms, conducted experiments, and led the writing of the paper. Changnan Xiao developed the mathematical framework and derived proofs. Tatsuya Konishi and Zixuan Ke contributed in discussions and helped edit the paper. Bing Liu supervised the project and helped write the paper.

### **Acknowledgements**

The work of Gyuhak Kim, Zixuan Ke and Bing Liu was supported in part by a research contract from KDDI, a research contract from DARPA (HR001120C0023), and three NSF grants (IIS-1910424, IIS-1838770, and CNS-2225427).

## Appendix A. Proof of Theorems and Corollaries

### Appendix A.1. Proof of Theorem 1

*Proof.* Since

$$\begin{aligned} H_{CIL}(x) &= H(y, \{\mathbf{P}(x \in \mathbf{X}_{k,j}|D)\}_{k,j}) \\ &= - \sum_{k,j} y_{k,j} \log \mathbf{P}(x \in \mathbf{X}_{k,j}|D) \\ &= - \log \mathbf{P}(x \in \mathbf{X}_{k_0,j_0}|D), \end{aligned}$$

$$\begin{aligned} H_{WP}(x) &= H(\tilde{y}, \{\mathbf{P}(x \in \mathbf{X}_{k_0,j}|x \in \mathbf{X}_{k_0}, D)\}_j) \\ &= - \sum_j y_{k_0,j} \log \mathbf{P}(x \in \mathbf{X}_{k_0,j}|x \in \mathbf{X}_{k_0}, D) \\ &= - \log \mathbf{P}(x \in \mathbf{X}_{k_0,j_0}|x \in \mathbf{X}_{k_0}, D), \end{aligned}$$

and

$$\begin{aligned} H_{TP}(x) &= H(\bar{y}, \{\mathbf{P}(x \in \mathbf{X}_k|D)\}_k) \\ &= - \sum_k \bar{y}_k \log \mathbf{P}(x \in \mathbf{X}_k|D) \\ &= - \log \mathbf{P}(x \in \mathbf{X}_{k_0}|D), \end{aligned}$$

we have

$$\begin{aligned} H_{CIL}(x) &= - \log \mathbf{P}(x \in \mathbf{X}_{k_0,j_0}|D) \\ &= - \log \mathbf{P}(x \in \mathbf{X}_{k_0,j_0}|x \in \mathbf{X}_{k_0}, D) - \log \mathbf{P}(x \in \mathbf{X}_{k_0}|D) \\ &= H_{WP}(x) + H_{TP}(x) \\ &\leq \epsilon + \delta. \end{aligned}$$

□

### Appendix A.2. Proof of Corollary 1.

*Proof.* By proof of Theorem 1, we have

$$H_{CIL}(x) = H_{WP}(x) + H_{TP}(x).$$

Taking expectations on both sides, we have i)

$$\begin{aligned} \mathbb{E}_{x \sim U(\mathbf{X})}[H_{CIL}(x)] &= \mathbb{E}_{x \sim U(\mathbf{X})}[H_{WP}(x)] + \mathbb{E}_{x \sim U(\mathbf{X})}[H_{TP}(x)] \\ &\leq \mathbb{E}_{x \sim U(\mathbf{X})}[H_{WP}(x)] + \delta. \end{aligned}$$

and ii)

$$\begin{aligned}\mathbb{E}_{x \sim U(\mathbf{X})}[H_{CIL}(x)] &= \mathbb{E}_{x \sim U(\mathbf{X})}[H_{WP}(x)] + \mathbb{E}_{x \sim U(\mathbf{X})}[H_{TP}(x)] \\ &\leq \epsilon + \mathbb{E}_{x \sim U(\mathbf{X})}[H_{TP}(x)].\end{aligned}$$

□

*Appendix A.3. Proof of Theorem 2.*

*Proof.* i) Assume  $x \in \mathbf{X}_{k_0}$ . For  $k = k_0$ , we have

$$\begin{aligned}H_{OOD,k_0}(x) &= -\log \mathbf{P}'_{k_0}(x \in \mathbf{X}_{k_0}|D) \\ &= -\log \mathbf{P}(x \in \mathbf{X}_{k_0}|D) \\ &= H_{TP}(x) \leq \delta.\end{aligned}$$

For  $k \neq k_0$ , we have

$$\begin{aligned}H_{OOD,k}(x) &= -\log \mathbf{P}'_k(x \notin \mathbf{X}_k|D) \\ &= -\log(1 - \mathbf{P}'_k(x \in \mathbf{X}_k|D)) \\ &= -\log(1 - \mathbf{P}(x \in \mathbf{X}_k|D)) \\ &= -\log \mathbf{P}(x \in \cup_{k' \neq k} \mathbf{X}_{k'}|D) \\ &\leq -\log \mathbf{P}(x \in \mathbf{X}_{k_0}|D) \\ &= H_{TP}(x) \leq \delta.\end{aligned}$$

ii) Assume  $x \in \mathbf{X}_{k_0}$ . For  $k = k_0$ , by  $H_{OOD,k_0}(x) \leq \delta_{k_0}$ , we have

$$-\log \mathbf{P}'_{k_0}(x \in \mathbf{X}_{k_0}|D) \leq \delta_{k_0},$$

which means

$$\mathbf{P}'_{k_0}(x \in \mathbf{X}_{k_0}|D) \geq e^{-\delta_{k_0}}.$$

For  $k \neq k_0$ , by  $H_{OOD,k}(x) \leq \delta_k$ , we have

$$-\log \mathbf{P}'_k(x \notin \mathbf{X}_k|D) \leq \delta_k,$$

which means

$$\mathbf{P}'_k(x \in \mathbf{X}_k|D) \leq 1 - e^{-\delta_k}.$$

Therefore, we have

$$\begin{aligned}
\mathbf{P}(x \in \mathbf{X}_{k_0} | D) &= \frac{\mathbf{P}'_{k_0}(x \in \mathbf{X}_{k_0} | D)}{\sum_{k'} \mathbf{P}'_{k'}(x \in \mathbf{X}_{k'} | D)} \\
&\geq \frac{e^{-\delta_{k_0}}}{1 + \sum_{k \neq k_0} 1 - e^{-\delta_k}} \\
&= \frac{e^{-\delta_{k_0}}}{e^{-\delta_{k_0}} + \sum_k 1 - e^{-\delta_k}} \\
&= \frac{1}{1 + e^{\delta_{k_0}} \sum_k 1 - e^{-\delta_k}}.
\end{aligned}$$

Hence,

$$\begin{aligned}
H_{TP}(x) &= -\log \mathbf{P}(x \in \mathbf{X}_{k_0} | D) \\
&\leq -\log \frac{1}{1 + e^{\delta_{k_0}} \sum_k 1 - e^{-\delta_k}} \\
&= \log[1 + e^{\delta_{k_0}} \sum_k 1 - e^{-\delta_k}] \\
&\leq e^{\delta_{k_0}} (\sum_k 1 - e^{-\delta_k}) \\
&= (\sum_k \mathbf{1}_{x \in \mathbf{X}_k} e^{\delta_k}) (\sum_k 1 - e^{-\delta_k}).
\end{aligned}$$

□

#### Appendix A.4. Proof of Theorem 3.

*Proof.* Using Theorem 1 and 2,

$$\begin{aligned}
H_{CIL}(x) &= -\log \mathbf{P}(x \in \mathbf{X}_{k_0, j_0} | D) \\
&= -\log \mathbf{P}(x \in \mathbf{X}_{k_0, j_0} | x \in \mathbf{X}_{k_0}, D) - \log \mathbf{P}(x \in \mathbf{X}_{k_0} | D) \\
&= H_{WP}(x) + H_{TP}(x) \\
&\leq \epsilon + H_{TP}(x) \\
&\leq \epsilon + (\sum_k \mathbf{1}_{x \in \mathbf{X}_k} e^{\delta_k}) (\sum_k 1 - e^{-\delta_k})
\end{aligned}$$

□



*Appendix A.5. Proof of Theorem 4.*

*Proof.* i) Assume  $x \in \mathbf{X}_{k_0, j_0} \subset \mathbf{X}_{k_0}$ . Define  $\mathbf{P}(x \in \mathbf{X}_{k, j} | x \in \mathbf{X}_k, D) = \mathbf{P}(x \in \mathbf{X}_{k, j} | D)$ . According to proof of Theorem 1,

$$\begin{aligned} H_{WP}(x) &= -\log \mathbf{P}(x \in \mathbf{X}_{k_0, j_0} | x \in \mathbf{X}_{k_0}, D), \\ H_{CIL}(x) &= -\log \mathbf{P}(x \in \mathbf{X}_{k_0, j_0} | D). \end{aligned}$$

Hence, we have

$$\begin{aligned} H_{WP}(x) &= -\log \mathbf{P}(x \in \mathbf{X}_{k_0, j_0} | x \in \mathbf{X}_{k_0}, D) \\ &= -\log \mathbf{P}(x \in \mathbf{X}_{k_0, j_0} | D) \\ &= H_{CIL}(x) \leq \eta. \end{aligned}$$

ii) Assume  $x \in \mathbf{X}_{k_0, j_0} \subset \mathbf{X}_{k_0}$ . Define  $\mathbf{P}(x \in \mathbf{X}_k | D) = \sum_j \mathbf{P}(x \in \mathbf{X}_{k, j} | D)$ . According to proof of Theorem 1,

$$\begin{aligned} H_{TP}(x) &= -\log \mathbf{P}(x \in \mathbf{X}_{k_0} | D), \\ H_{CIL}(x) &= -\log \mathbf{P}(x \in \mathbf{X}_{k_0, j_0} | D). \end{aligned}$$

Hence, we have

$$\begin{aligned} H_{TP}(x) &= -\log \mathbf{P}(x \in \mathbf{X}_{k_0} | D) \\ &= -\log \sum_j \mathbf{P}(x \in \mathbf{X}_{k_0, j} | D) \\ &\leq -\log \mathbf{P}(x \in \mathbf{X}_{k_0, j_0} | D) \\ &= H_{CIL}(x) \leq \eta. \end{aligned}$$

iii) Assume  $x \in \mathbf{X}_{k_0, j_0} \subset \mathbf{X}_{k_0}$ . Define  $\mathbf{P}'_i(x \in \mathbf{X}_k | D) = \mathbf{P}(x \in \mathbf{X}_k | D) = \sum_j \mathbf{P}(x \in \mathbf{X}_{k, j} | D)$ . According to proof of Theorem 4 ii), we have

$$H_{TP}(x) \leq \eta.$$

According to proof of Theorem 2 i), we have

$$H_{OOD, i}(x) \leq H_{TP}(x).$$

Therefore,

$$H_{OOD, i}(x) \leq H_{TP}(x) \leq \eta.$$

□

## Appendix B. Additional Results and Explanation Regarding Table 1 in the Main Paper

In Section 4.2.3, we showed that a better OOD detection improves CIL performance. For the post-processing method ODIN, we only reported the results on C100-10T. Table B.9 shows the results on the other datasets.

A continual learning method with a better AUC shows a better CIL performance than other methods with lower AUC. For instance, original HAT achieves AUC of 82.47 while HyperNet achieves 78.54 on C10-5T. The CIL for HAT is 62.67 while it is 53.40 for HyperNet. However, there are some exceptions that this comparison does not hold. An example is LwF. Its AUC and CIL are 89.39 and 54.67 on C10-5T. Although its AUC is better than HAT, the CIL is lower. This is due to the fact that CIL improves with WP and TP according to Theorem 1. The contraposition of Theorem 4 also says if the cross-entropy of TIL is large, that of CIL is also large. Indeed, the average within-task prediction (WP) accuracy for LwF on C10-5T is 95.2 while the same for HAT is 96.7. Improving WP is also important in achieving good CIL performances.

For PASS, we had to tune  $\tau_k$  using a validation set. This is because the softmax in Eq. 22 improves AUC by making the IND (in-distribution) and OOD scores more separable within a task, but deteriorates the final scores across tasks. To be specific, the test instances are predicted as one of the classes in the first task after softmax because the relative values between classes in task 1 is larger than the other tasks in PASS. Therefore, larger  $\tau_1$  and smaller  $\tau_k$ , for  $k > 1$ , are chosen to compensate the relative values.

## Appendix C. Definitions of TP

As noted in the main paper, the class prediction in Eq. 2 varies by definition of WP and TP. The precise definition of WP and TP depends on implementation. Due to this subjectivity, we follow the prediction method in the existing approaches in continual learning, which is the arg max over the output. In this section, we show that the arg max over output is a special case of Eq. 2. We also provide CIL results using different definitions of TP.

We first establish another theorem. This is an extension of Theorem 2 and connects the standard prediction method to our analysis.

Table B.9: Performance Comparison between the Original Output and ODIN

Method	CIL	C10-5T		C100-20T		T-5T		T-10T	
		AUC	CIL	AUC	CIL	AUC	CIL	AUC	CIL
OWM	Original	81.33	51.79	71.90	24.15	58.49	10.00	59.48	8.57
	ODIN	71.72	40.65	68.52	23.05	58.46	10.77	59.38	9.52
MUC	Original	79.49	52.85	66.20	14.19	68.42	33.57	62.63	17.39
	ODIN	79.54	53.22	65.72	14.11	68.32	33.45	62.17	17.27
PASS	Original	66.51	47.34	70.26	24.99	65.18	28.40	63.27	19.07
	ODIN	63.08	35.20	69.81	21.83	65.93	29.03	62.73	17.78
LwF	Original	89.39	54.67	89.84	44.33	78.20	32.17	79.43	24.28
	ODIN	88.94	63.04	88.68	47.56	76.83	36.20	77.02	28.29
A-GEM	Original	85.93	20.03	74.48	4.14	72.33	13.52	76.42	7.66
	ODIN	86.43	34.03	75.12	6.99	72.46	14.69	76.75	8.50
EEIL	Original	89.72	57.09	85.96	33.46	64.82	14.67	64.87	9.79
	ODIN	89.20	59.47	85.46	35.16	57.01	11.92	55.42	6.88
GD	Original	91.23	58.69	86.76	38.83	68.63	16.36	69.61	11.73
	ODIN	90.39	60.53	86.64	42.33	60.75	13.43	63.92	11.83
BiC	Original	90.89	61.41	89.46	48.92	80.17	41.75	80.37	33.77
	ODIN	91.86	64.29	87.89	47.40	74.54	37.40	76.27	29.06
DER++	Original	90.16	66.04	85.44	46.59	71.80	35.80	72.41	30.49
	ODIN	87.08	63.07	87.72	49.26	73.92	37.87	72.91	32.52
HAL	Original	86.16	32.82	65.59	13.51	53.00	3.42	57.87	3.36
	ODIN	76.27	44.75	64.46	17.40	53.26	4.80	58.13	4.74
HAT	Original	82.47	62.67	75.35	25.64	72.28	38.46	71.82	29.78
	ODIN	82.45	62.60	75.36	25.84	72.31	38.61	71.83	30.01
HyperNet	Original	78.54	53.40	72.04	18.67	54.58	7.91	55.37	5.32
	ODIN	79.39	56.72	73.89	23.8	54.60	8.64	55.53	6.91
Sup	Original	79.16	62.37	81.14	34.70	74.13	41.82	74.59	36.46
	ODIN	82.38	62.63	81.48	36.35	73.96	41.10	74.61	36.46

Performance comparison between the original output and output post-processed with OOD detection technique ODIN. Note that ODIN is not applicable to iCaRL and Mnemonics as they are not based on softmax but some distance functions. The result for C100-10T are reported in the main paper.

**Theorem 5** (Extension of Theorem 2). *i) If  $H_{TP}(x) \leq \delta$ , let  $\mathbf{P}'_k(x \in \mathbf{X}_k|D) = \mathbf{P}(x \in \mathbf{X}_k|D)^{1/\tau_k}$ ,  $\forall \tau_k > 0$ , then  $H_{OOD,k}(x) \leq \max(\delta/\tau_k, -\log(1 - (1 - e^{-\delta})^{1/\tau_k}))$ ,  $\forall k = 1, \dots, T$ .*

*ii) If  $H_{OOD,k}(x) \leq \delta_k$ ,  $k = 1, \dots, T$ , let  $\mathbf{P}(x \in \mathbf{X}_k|D) = \frac{\mathbf{P}'_k(x \in \mathbf{X}_k|D)^{1/\tau_k}}{\sum_j \mathbf{P}'_j(x \in \mathbf{X}_j|D)^{1/\tau_j}}$ ,  $\forall \tau_k > 0$ , then  $H_{TP}(x) \leq \sum_k \frac{\mathbf{1}_{x \in \mathbf{X}_k} \delta_k}{\tau_k} + \frac{\sum_k (1 - e^{-\delta_k})^{1/\tau_k}}{\sum_k \mathbf{1}_{x \in \mathbf{X}_k} (1 - (1 - e^{-\delta_k})^{1/\tau_k})}$ , where  $\mathbf{1}_{x \in \mathbf{X}_k}$  is an indicator function.*

In Theorem 5 (proof appears later), we can observe that  $\delta/\tau_k$  decreases with the increase of  $\tau_k$ , while  $-\log(1 - (1 - e^{-\delta})^{1/\tau_k})$  increases. Hence, when TP is given, let  $\delta = H_{TP}(x)$ , we can find the optimal  $\tau_i$  to define OOD by solving  $\delta/\tau_k = -\log(1 - (1 - e^{-\delta})^{1/\tau_k})$ . Similarly, given OOD, let  $\delta_k = H_{OOD,k}(x)$ , we can find the optimal  $\tau_1, \dots, \tau_T$  to define TP by finding the global minima of  $\sum_k \frac{\mathbf{1}_{x \in \mathbf{X}_k} \delta_k}{\tau_k} + \frac{\sum_k (1 - e^{-\delta_k})^{1/\tau_k}}{\sum_k \mathbf{1}_{x \in \mathbf{X}_k} (1 - (1 - e^{-\delta_k})^{1/\tau_k})}$ . The optimal  $\tau_k$  can be found using a memory buffer to save a small number of previous data like that in a replay-based continual learning method.

In Theorem 5 (ii), let  $\mathbf{P}'_k(x \in \mathbf{X}_k|D) = \sigma(\max f(x)_k)$ , where  $\sigma$  is the sigmoid and  $f(x)_k$  is the output of task  $k$  and choose  $\tau_k \approx 0$  for each  $k$ . Then  $\mathbf{P}(x \in \mathbf{X}_k|D)$  becomes approximately 1 for the task  $k$  where the maximum logit value appears and 0 for the rest tasks. Therefore, Eq. 2 in the paper

$$\mathbf{P}(x \in \mathbf{X}_{k,j}|D) = \mathbf{P}(x \in \mathbf{X}_{k,j}|x \in \mathbf{X}_k, D)\mathbf{P}(x \in \mathbf{X}_k|D)$$

is zero for all classes in tasks  $k' \neq k$ . Since only the probabilities of classes in task  $k$  are non-zero, taking arg max over all class probabilities gives the same class as arg max over output logits.

We have also tried another definition of WP and TP. The considered WP is

$$\mathbf{P}(x \in \mathbf{X}_{k,j}|x \in \mathbf{X}_k, D) = \frac{e^{f(x)_{kj}/\nu_k}}{\sum_j e^{f(x)_{kj}/\nu_k}}, \quad (\text{C.1})$$

where  $\nu_k$  is a temperature scaling parameter for task  $k$ , and the TP is

$$\mathbf{P}(x \in \mathbf{X}_k|D) = \frac{\mathbf{P}'_k(x \in \mathbf{X}_k|D)}{\sum_k \mathbf{P}'_k(x \in \mathbf{X}_k|D)}, \quad (\text{C.2})$$

where  $\mathbf{P}'_k(x \in \mathbf{X}_k|D) = \max_j e^{f(x)_{kj}/\tau_k} / \sum_j e^{f(x)_{kj}/\tau_k}$  and  $\tau_k$  is a temperature scaling parameter. This is the maximum softmax of task  $k$ . We choose

Table C.10: Average Accuracy with a Different Prediction Method

Method	C10-5T	C100-10T	C100-20T	T-5T	T-10T
<i>OWM</i>	40.6±0.47	28.6±0.82	22.9±0.32	10.4±0.54	9.2±0.35
<i>MUC</i>	53.2±1.32	30.6±1.21	14.0±0.12	33.1±0.18	17.2±0.13
<i>PASS</i> <sup>†</sup>	33.6±0.71	18.5±1.85	20.8±0.85	21.4±0.44	13.0±0.55
LwF	63.0±0.34	51.9±0.88	47.5±0.62	35.9±0.32	27.8±0.29
iCaRL*	65.3±0.83	52.9±0.39	48.2±0.70	34.8±0.34	27.3±0.17
A-GEM	34.0±1.86	14.5±0.55	7.3±1.78	15.4±0.24	9.0±0.30
EEIL	59.5±0.41	41.8±0.78	37.9±6.11	15.1±0.00	7.5±0.19
GD	68.0±0.75	47.2±0.33	41.8±0.25	15.7±2.08	12.2±0.14
Mnemonics <sup>†*</sup>	65.6±1.55	50.7±0.72	47.9±0.71	36.3±0.30	27.7±0.78
BiC	65.5±0.81	50.8±0.69	47.2±0.71	37.0±0.58	29.1±0.34
DER++	63.1±1.12	54.6±1.21	48.9±1.18	37.4±0.72	32.1±0.44
HAL	43.0±3.10	20.0±1.15	17.0±0.83	4.6±0.58	4.8±0.50
<i>HAT</i>	62.6±1.31	41.5±0.80	25.9±0.56	38.9±1.62	30.1±0.52
<i>HyperNet</i>	56.7±1.23	32.4±1.07	24.5±1.12	8.9±0.58	7.0±0.52
<i>Sup</i>	62.6±1.11	46.8±0.34	36.0±0.32	41.5±1.17	35.7±0.40
<i>HAT+CSI</i>	85.2±0.92	62.9±1.07	53.6±0.84	47.0±0.38	46.2±0.30
<i>Sup+CSI</i>	87.4±0.40	66.6±0.23	60.5±0.89	47.7±0.30	46.3±0.30
HAT+CSI+c	85.2±0.94	63.6±0.69	55.4±0.79	51.4±0.38	46.5±0.26
Sup+CSI+c	86.2±0.79	67.0±0.14	60.4±1.04	48.2±0.35	46.1±0.32

Average classification accuracy. The results are based on class prediction method defined with WP and TP in Eq. C.1 and Eq. C.2, respectively. The results can improve by finding optimal temperature scaling parameters.

$\nu_k = 0.1$  and  $\tau_k = 5$  for all  $k$ . A good  $\tau$  and  $\nu$  can be found using grid search on a validation set. However, one can also find the optimal values by optimization using some past data saved for memory buffer. The CIL results for the new prediction method is in Table C.10.

*Proof of Theorem 5.* i) Assume  $x \in \mathbf{X}_{k_0}$ .

For  $k = k_0$ , we have

$$\begin{aligned}
H_{OOD,k_0}(x) &= -\log \mathbf{P}'_{k_0}(x \in \mathbf{X}_{k_0} | D) \\
&= -\frac{1}{\tau_{k_0}} \log \mathbf{P}(x \in \mathbf{X}_{k_0} | D) \\
&= \frac{1}{\tau_{k_0}} H_{TP}(x) \leq \frac{\delta}{\tau_{k_0}}.
\end{aligned}$$

For  $k \neq k_0$ , we have

$$\begin{aligned}
H_{OOD,k}(x) &= -\log \mathbf{P}'_k(x \notin \mathbf{X}_k | D) \\
&= -\log(1 - \mathbf{P}'_k(x \in \mathbf{X}_k | D)) \\
&= -\log(1 - \mathbf{P}(x \in \mathbf{X}_k | D)^{1/\tau_k}) \\
&= -\log(1 - (1 - \mathbf{P}(x \in \cup_{k' \neq k} \mathbf{X}_{k'} | D))^{1/\tau_k}) \\
&\leq -\log(1 - (1 - \mathbf{P}(x \in \mathbf{X}_{k_0} | D))^{1/\tau_k}) \\
&= -\log(1 - (1 - e^{-H_{TP}(x)})^{1/\tau_k}) \\
&\leq -\log(1 - (1 - e^{-\delta})^{1/\tau_k}).
\end{aligned}$$

ii) Assume  $x \in \mathbf{X}_{k_0}$ .

For  $k = k_0$ , by  $H_{OOD,k_0}(x) \leq \delta_{k_0}$ , we have

$$-\log \mathbf{P}'_{k_0}(x \in \mathbf{X}_{k_0} | D) \leq \delta_{k_0},$$

which means

$$\mathbf{P}'_{k_0}(x \in \mathbf{X}_{k_0} | D) \geq e^{-\delta_{k_0}}.$$

For  $k \neq k_0$ , by  $H_{OOD,k}(x) \leq \delta_k$ , we have

$$-\log \mathbf{P}'_k(x \notin \mathbf{X}_k | D) \leq \delta_k,$$

which means

$$\mathbf{P}'_k(x \in \mathbf{X}_k | D) \leq 1 - e^{-\delta_k}.$$

Therefore, we have

$$\begin{aligned}
\mathbf{P}(x \in \mathbf{X}_{k_0} | D) &= \frac{\mathbf{P}'_{k_0}(x \in \mathbf{X}_{k_0} | D)^{1/\tau_{k_0}}}{\sum_k \mathbf{P}'_k(x \in \mathbf{X}_k | D)^{1/\tau_k}} \\
&\geq \frac{e^{-\delta_{k_0}/\tau_{k_0}}}{1 + \sum_{k \neq k_0} (1 - e^{-\delta_k})^{1/\tau_k}} \\
&= \frac{e^{-\delta_{k_0}/\tau_{k_0}}}{1 - (1 - e^{-\delta_{k_0}})^{1/\tau_{k_0}} + \sum_k (1 - e^{-\delta_k})^{1/\tau_k}} \\
&= \frac{e^{-\delta_{k_0}/\tau_{k_0}}}{1 - (1 - e^{-\delta_{k_0}})^{1/\tau_{k_0}}} \cdot \frac{1}{1 + \frac{\sum_k (1 - e^{-\delta_k})^{1/\tau_k}}{1 - (1 - e^{-\delta_{k_0}})^{1/\tau_{k_0}}}}.
\end{aligned}$$

Hence,

$$\begin{aligned}
H_{TP}(x) &= -\log \mathbf{P}(x \in \mathbf{X}_{k_0} | D) \\
&\leq -\log \frac{e^{-\delta_{k_0}/\tau_{k_0}}}{1 - (1 - e^{-\delta_{k_0}})^{1/\tau_{k_0}}} \cdot \frac{1}{1 + \frac{\sum_k (1 - e^{-\delta_k})^{1/\tau_k}}{1 - (1 - e^{-\delta_{k_0}})^{1/\tau_{k_0}}}} \\
&= \frac{\delta_{k_0}}{\tau_{k_0}} + \log[1 - (1 - e^{-\delta_{k_0}})^{1/\tau_{k_0}}] + \log \left[ 1 + \frac{\sum_k (1 - e^{-\delta_k})^{1/\tau_k}}{1 - (1 - e^{-\delta_{k_0}})^{1/\tau_{k_0}}} \right] \\
&\leq \frac{\delta_{k_0}}{\tau_{k_0}} + \frac{\sum_k (1 - e^{-\delta_k})^{1/\tau_k}}{1 - (1 - e^{-\delta_{k_0}})^{1/\tau_{k_0}}} \\
&= \sum_k \frac{\mathbf{1}_{x \in \mathbf{X}_k} \delta_k}{\tau_k} + \frac{\sum_k (1 - e^{-\delta_k})^{1/\tau_k}}{\sum_k \mathbf{1}_{x \in \mathbf{X}_k} (1 - (1 - e^{-\delta_k})^{1/\tau_k})}.
\end{aligned}$$

□

## Appendix D. Output Calibration

In this section, we discuss the output calibration technique used in Section 4.2.4 to improve the final prediction accuracy. Even if an OOD detection of each task was perfect (i.e. the model accepts and rejects IND and OOD samples perfectly), the system could make incorrect class prediction if the magnitudes of outputs across different tasks are different. To ensure that the output values are comparable, we calibrate the outputs by scaling  $\alpha_k$  and shifting  $\beta_k$  for each task. The optimal parameters  $(\alpha_k, \beta_k) \in R \times R$  can be found by solving optimization problem using samples in memory buffer. More precisely, denote the memory buffer  $\mathcal{M}$  and calibration parameters  $(\alpha, \beta) \in R^T \times R^T$ , where  $T$  is the number of learned tasks. After training  $T$ th task, we find optimal calibration parameters by minimizing the cross-entropy loss,

$$\mathcal{L} = -\frac{1}{|\mathcal{M}|} \sum_{(x,y) \in \mathcal{M}} \log p(y|x) \tag{D.1}$$

where  $p(c|x)$  is computed using the softmax,

$$\text{softmax} \bigoplus [\alpha_k f(x)_k + \beta_k] \tag{D.2}$$

where  $\oplus$  indicates the concatenation and  $f(x)_k$  is the output of task  $k$  as Eq. 21. Given the optimal parameters  $(\alpha^*, \beta^*)$ , we make final prediction as

$$\hat{y} = \arg \max \bigoplus [\alpha_k^* f(x)_k + \beta_k^*] \quad (\text{D.3})$$

If we use  $OOD_k = \sigma(\alpha_k^* f(x)_k + \beta_k^*)$ , where  $\sigma$  is the sigmoid, and  $TP_k = OOD_k / \sum_{k'} OOD_{k'}$ , the theoretical results in Section 3 hold.

## Appendix E. TIL (WP) Results

The TIL (WP) results of all the systems are reported in Table E.11. HAT and Sup show strong performances compared to the other baselines as they leverage task-specific parameters. However, as shown in Theorem 1, the CIL depends on TP (or OOD). Without an OOD detection mechanism in HAT or Sup, they perform poorly in CIL as shown in the main paper. The contrastive learning in CSI also improves the IND prediction (i.e., WP), and this along with OOD detection results in the strong CIL performance.

## Appendix F. Hyper-parameters

Here we report the hyper-parameters that we did not report in the main paper due to space limitations. We mainly report the hyper-parameters of the proposed methods, HAT+CSI, Sup+CSI, and their calibrated versions. For all the experiments of the proposed methods, we use the values chosen by the original CSI [58]. We use LARS [66] optimization with learning rate 0.1 for training the feature extractor. We linearly increase the learning rate by 0.1 per epoch for the first 10 epochs. After that, we use cosine scheduler [42] without restart as in [58, 13]. After training the feature extractor, we train the linear classifier for 100 epochs with SGD with learning rate 0.1 and reduce the rate by 0.1 at 60, 75, and 90 epochs. For all the experiments except MNIST, we train the feature extractor for 700 epochs with batch size 128.

For the following hyper-parameters, we use 10% of training data for validation to find a good set of values. For the number of epochs and batch size for MNIST, Sup+CSI trains for 1000 epochs with batch size of 32 while HAT+CSI trains for 700 epochs with batch size of 256. The hard attention regularization penalty  $\lambda_i$  in HAT is different by experiments and task  $i$ . For MNIST, we use  $\lambda_1 = 0.25$ , and  $\lambda_2 = \dots = \lambda_5 = 0.1$ . For



Table E.11: The TIL Results of All the Systems.

Method	C10-5T	C100-10T	C100-20T	T-5T	T-10T	Avg.
<i>OWM</i>	85.0±0.07	59.6±0.83	65.4±0.48	22.4±0.87	28.1±0.55	52.1
<i>MUC</i>	95.1±0.10	77.3±0.83	73.4±9.16	55.9±0.26	47.2±0.22	69.8
<i>PASS</i> <sup>†</sup>	83.8±0.68	72.1±0.70	76.8±0.32	49.9±0.56	46.5±0.39	65.8
LwF	95.2±0.30	86.2±1.00	89.0±0.45	56.4±0.48	55.3±0.35	76.4
iCaRL	94.9±0.34	84.2±1.04	85.7±0.68	54.5±0.29	52.7±0.37	74.4
A-GEM	82.5±4.19	58.9±2.14	56.4±7.03	32.1±0.90	30.1±0.29	52.0
EEIL	93.4±0.02	83.1±3.13	88.4±2.07	30.3±0.89	25.9±0.04	64.2
GD	94.4±0.09	82.2±0.18	85.7±0.20	30.7±1.79	32.2±0.37	65.0
Mnemonics <sup>†*</sup>	94.5±0.46	82.3±0.30	86.2±0.46	54.8±0.16	52.9±0.66	74.1
BiC	95.4±0.35	84.6±0.48	88.7±0.19	61.5±0.60	62.2±0.45	78.5
DER++	92.0±0.54	84.0±9.43	86.6±9.44	57.4±1.31	60.0±0.74	76.0
HAL	82.8±1.94	49.5±1.51	61.1±1.43	13.2±0.77	21.2±0.41	26.2
<i>HAT</i>	96.7±0.18	84.0±0.23	85.0±0.98	61.2±0.72	63.8±0.41	78.1
<i>HyperNet</i>	94.6±0.37	76.8±1.22	83.5±0.98	23.9±0.60	28.0±0.69	61.4
<i>Sup</i>	96.6±0.21	87.9±0.27	91.6±0.15	64.3±0.24	68.4±0.22	81.8
<i>HAT+CSI</i>	98.7±0.06	92.0±0.37	94.3±0.06	68.4±0.16	72.4±0.21	85.2
<i>Sup+CSI</i>	98.7±0.07	93.0±0.13	95.3±0.20	65.9±0.25	74.1±0.28	85.4

The calibrated versions (+c) of our methods are omitted as calibration does not affect TIL performance. Exemplar-free methods are italicized. The last column Avg. shows the average TIL accuracy of each method over all datasets.

C10-5T, we use  $\lambda_1 = 1.0$ , and  $\lambda_2 = \dots = \lambda_5 = 0.75$ . For C100-10T,  $\lambda_1 = 1.5$ , and  $\lambda_2 = \dots = \lambda_{10} = 1.0$  are used. For C100-20T,  $\lambda_1 = 3.5$ , and  $\lambda_2 = \dots = \lambda_{20} = 2.5$  are used. For T-5T,  $\lambda_i = 0.75$  for all tasks, and lastly, for T-10T,  $\lambda_1 = 1.0$ , and  $\lambda_2 = \dots = \lambda_{10} = 0.75$  are used. We use larger  $\lambda_1$  for the first task than the later tasks as we have found that the larger regularization on the first task results in better accuracy. This is by the definition of regularization in HAT. The earlier task gives lower penalty than later tasks. We manually give larger penalty to the first task. We did not search hyper-parameter  $\lambda_t$  for tasks  $t \geq 2$ . For sparsity in Sup+CSI, we simply choose the least sparsity value of 32 used in the original Sup paper without parameter search.

Calibration methods (HAT+CSI+c and Sup+CSI+c) are based on its memory free versions (i.e. HAT+CSI and Sup+CSI). Therefore, the model training part uses the same hyper-parameters as their calibration free counterparts. For calibration training, we use SGD with learning rate 0.01, 160 training iterations, and batch size of 15 for HAT+CSI+c for all experiments.

For Sup+CSI+c, we use the same values for all the experiments except for MNIST. For MNIST, we use learning rate 0.05, batch size of 8, and run 280 iterations.

For the baselines, we use the hyper-parameters reported in the original papers or in their code. If the hyper-parameters are unknown or the code does not reproduce the result (e.g., the baseline did not implement a particular dataset or the code had undergone significant version change), we search for the hyper-parameters as we did for HAT+CSI and Sup+CSI.

### Appendix G. Forgetting Rate

We discuss forgetting rate (i.e., backward transfer) [41], which is defined for task  $t$  as

$$\mathcal{F}^t = \frac{1}{t-1} \sum_{k=1}^{t-1} \mathcal{A}_k^{\text{init}} - \mathcal{A}_k^t, \tag{G.1}$$

where  $\mathcal{A}_k^{\text{init}}$  is the classification accuracy of task  $k$ 's data after learning it for the first time and  $\mathcal{A}_k^t$  is the accuracy of task  $k$ 's data after learning task  $t$ . We report the forgetting rate after learning the last task.

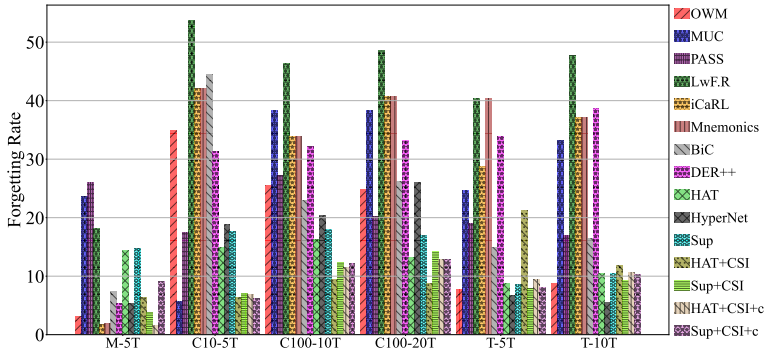


Figure G.4: Average forgetting rate (%). The lower the value, the better the method is on forgetting.

Figure G.4 shows the forgetting rates of each method. Some methods (e.g., OWM, iCaRL) experience less forgetting than the proposed methods HAT+CSI and Sup+CSI on M-5T. On this dataset, all the systems performed well. For instance, OWM and iCaRL achieve 95.8% and 96.0% accuracy while HAT+CSI and HAT+CSI+c achieve 94.4 and 96.9% accuracy. As we have

noted in the main paper, Sup+CSI and Sup+CSI+c achieve only 80.7 and 81.0 on M-5T although they have improved drastically from 70.1% of the base method Sup.

OWM and HyperNet show lower forgetting rates than HAT+CSI+c and Sup+CSI+c on T-5T and T-10T. However, they are not able to adapt to new classes as OWM and HyperNet achieve the classification accuracy of only 10.0% and 7.9%, respectively, on T-5T and 8.6% and 5.3% on T-10T. HAT+CSI+c and Sup+CSI+c achieves 51.7% and 49.2%, respectively, on T-5T and 47.6% and 46.2% on T-10T.

In fact, the performance reduction (i.e., forgetting) in our proposed methods occurs not because the systems forget the previous task knowledge, but because the systems learn more classes and the classification naturally becomes harder. The continual learning mechanisms (HAT and Sup) used in the proposed methods experience little or no forgetting because they find independent subset of parameters for each task, and the learned parameters are not interfered during training. For the forgetting rate results in the TIL setting, refer to our earlier workshop paper [28].

## Appendix H. Pseudo-Code

For task  $k$ , Let  $p(y|\mathbf{x}, k) = \text{softmax}f(h(\mathbf{x}, k; \theta, \mathbf{e}^k); \phi_k)$ , where  $\theta$  is the parameters for adapter,  $\mathbf{e}^k$  is the trainable embedding for hard attentions, and  $\phi_k$  is the set of parameters of the classification head of task  $k$ . Algorithm 1 and Algorithm 2 describe the training and testing processes, respectively. We add comments with the symbol “//”.

---

**Algorithm 1** Training MORE

---

**Require:** Memory  $\mathcal{M}$ , learning rate  $\lambda$ , a sequence of tasks  $\mathcal{D} = \{\mathcal{D}^k\}_{k=1}$ , and parameters  $\{\theta, \mathbf{e}, \phi\}$ , where  $\mathbf{e}$  and  $\phi$  are collections of task embeddings  $\mathbf{e}^k$  and task heads  $\phi_k$

// CL starts

- 1: **for** each task data  $\mathcal{D}^k \in \mathcal{D}$  **do**
  - // Model training
  - 2: **for** a batch  $(\mathbf{X}_i^k, \mathbf{y})$  in  $\mathcal{D}^k$ , until converge **do**
  - 3:  $\mathbf{X}_s = \text{sample}(\mathcal{M})$
  - 4: Compute loss (Eq. 24+Eq. 13) and gradients of parameters
  - 5: Modify the model parameters  $\nabla\theta \leftarrow \nabla\theta'$  using Eq. 11
  - 6: Update parameters as  $\theta \leftarrow \theta - \lambda\nabla\theta$ ,  $\mathbf{e}^k \leftarrow \mathbf{e}^k - \lambda\partial\mathcal{L}$ ,  $\phi_k \leftarrow \phi_k - \lambda\partial\mathcal{L}$
  - 7: **end for**
    - // Back-updating in Section 5.1.2
    - 8: Randomly select  $\tilde{\mathcal{D}} \subset \mathcal{D}^k$ , where  $|\tilde{\mathcal{D}}| = |\mathcal{M}|$
    - 9: **for** each task  $j$ , until converge **do**
    - 10: minimize  $\mathcal{L}(\phi_j)$  of Eq. 26
    - 11: **end for**
      - // Obtain statistics in Section 5.1.3
      - 12: Compute  $\boldsymbol{\mu}_j^k$  using Eq. 28 and  $\mathbf{S}^k$  using Eq. 29
      - 13: **end for**

---

---

**Algorithm 2** MORE Prediction

---

**Require:** Test instance  $\mathbf{x}$  and parameters  $\{\theta, \mathbf{e}, \phi\}$

- 1: **for** each task  $k$  **do**
- 2: Obtain  $p(\mathcal{Y}^k|\mathbf{x}, k)$
- 3: Obtain  $s^k(\mathbf{x})$  using Eq. 27
- 4: **end for**
  - // Concatenate outputs for final prediction  $y$  and OOD score  $s$
  - 5:  $y = \arg \max \bigoplus_{1 \leq k \leq t} p(\mathcal{Y}^k|\mathbf{x}, k) s^k(\mathbf{x})$  (i.e. Eq. 30)
  - 6:  $s = \max \bigoplus_{1 \leq k \leq t} p(\mathcal{Y}^k|\mathbf{x}, k) s^k(\mathbf{x})$

---

Table I.12: Required Memory

Method	C10-5T	C100-10T	C100-20T	T-5T	T-10T
OWM	26.6M	28.1M	28.1M	28.2M	28.2M
MUC	22.9M	24.1M	24.1M	24.1M	24.1M
PASS	22.9M	24.2M	24.2M	24.3M	24.4M
LwF	22.9M	24.1M	24.1M	24.1M	24.1M
iCaRL	22.9M	24.1M	24.1M	24.1M	24.1M
A-GEM	26.5M	31.4M	31.4M	31.5M	31.5M
EEIL	22.9M	24.1M	24.1M	24.1M	24.1M
GD	22.9M	24.1M	24.1M	24.1M	24.1M
BiC	22.9M	24.1M	24.1M	24.1M	24.1M
DER++	22.9M	24.1M	24.1M	24.1M	24.1M
HAL	22.9M	24.1M	24.1M	24.1M	24.1M
HAT	23.0M	24.7M	25.4M	24.6M	25.1M
Sup	24.7M	33.7M	45.7M	27.7M	33.7M
MORE	23.7M	25.9M	27.7M	25.1M	25.9M

Total memory (in entries) required for each method without the replay memory buffer.

## Appendix I. Size of Memory Required

In this section, we report sizes of memory required by each method in Section 5.2. The sizes include network size, replay buffer, all other parameters or example kept in memory simultaneously for a model to be functional.

We use an ‘entry’ to refer to a parameter or element in a vector or matrix to calculate the total memory required to train and test. The pre-trained backbone uses 21.6 million (M) entries (parameters). The adapter modules use 1.2M entries for CIFAR10 and 2.4M for other datasets. The baselines and our method use 22.9M and 24.1M entries for the model on CIFAR10 and other datasets, respectively. The unique technique of each method may add additional entries for training and test/inference.

The total memory required for each method without considering the replay memory buffer is reported in Table I.12. Our method is competitive in memory consumption. Baselines such as OWM and A-GEM take considerably more memory than our system. iCaRL and DER++ take the least amount of memory, but the differences between our method and theirs are only 0.8M, 1.8M, 3.6M, 1.0M, and 1.8M for C10-5T, C100-10T, C100-20T, T-5T and T-10T.

Many replay based methods (e.g., iCaRL, HAL) need to save the previous network for distillation during training. This requires additional 1.2M or

2.4M entries for CIFAR10 or other datasets. Our method does not save the previous model as we do not use distillation.

Note that a large memory consumption usually comes from the memory buffer as the raw data is of size  $32*32*3$  or  $64*64*3$  for CIFAR and T-ImageNet. For memory buffer of size 2000, a system needs 6.1M or 24.6M entries for CIFAR or T-ImageNet. Therefore, saving a smaller number of samples is important for reducing the memory consumption. As we demonstrated in Table 5 and Table 6 in the main paper, our method performs better than the baselines even with a smaller memory buffer. In Table 5, we use large memory sizes (e.g., 200 and 2000 for CIFAR10 and other datasets). In Table 6, we reduce the memory size by half. When we compare the accuracy of our method in Table 6 to those of the baselines in Table 5, our method still outperforms them on all datasets. Our method with a smaller memory buffer achieves average classification accuracy of 88.13, 71.69, 71.29, 64.17, 61.90 on C10-5T, C100-10T, C100-20T, T-5T, and T-10T. On the other hand, the best baselines achieve 88.98, 69.73, 70.03, 61.03, 58.34 on the same experiments with a larger memory buffer.

## References

- [1] Abati, D., Tomczak, J., Blankevoort, T., Calderara, S., Cucchiara, R., Bejnordi, E., 2020. Conditional channel gated networks for task-aware continual learning, in: CVPR, pp. 3931–3940.
- [2] Aljundi, R., Belilovsky, E., Tuytelaars, T., Charlin, L., Caccia, M., Lin, M., Caccia, L., 2019. Online continual learning with maximal interfered retrieval, in: NeurIPS.
- [3] Aljundi, R., Chakravarty, P., Tuytelaars, T., 2016. Expert gate: Lifelong learning with a network of experts. CoRR, abs/1611.06194 2.
- [4] Ayub, A., Wagner, A., 2021. {EEC}: Learning to encode and regenerate images for continual learning, in: International Conference on Learning Representations. URL: <https://openreview.net/forum?id=1Waz5a91cFU>.
- [5] Bang, J., Kim, H., Yoo, Y., Ha, J.W., Choi, J., 2021. Rainbow memory: Continual learning with a memory of diverse samples, in: Proceedings of the IEEE/CVF Conference on Computer Vision and Pattern Recognition, pp. 8218–8227.

- [6] Bendale, A., Boulton, T., 2015. Towards open world recognition, in: Proceedings of the IEEE conference on computer vision and pattern recognition, pp. 1893–1902.
- [7] Buzzega, P., Boschini, M., Porrello, A., Abati, D., CALDERARA, S., 2020. Dark experience for general continual learning: a strong, simple baseline, in: NeurIPS.
- [8] Castro, F.M., Marín-Jiménez, M.J., Guil, N., Schmid, C., Alahari, K., 2018. End-to-end incremental learning, in: Proceedings of the European conference on computer vision (ECCV).
- [9] Cha, H., Lee, J., Shin, J., 2021. Co2l: Contrastive continual learning, in: ICCV.
- [10] Chaudhry, A., Gordo, A., Dokania, P., Torr, P., Lopez-Paz, D., 2021. Using hindsight to anchor past knowledge in continual learning. Proceedings of the AAAI Conference on Artificial Intelligence 35, 6993–7001. URL: <https://ojs.aaai.org/index.php/AAAI/article/view/16861>.
- [11] Chaudhry, A., Ranzato, M., Rohrbach, M., Elhoseiny, M., 2018. Efficient lifelong learning with a-gem. arXiv preprint arXiv:1812.00420 .
- [12] Chaudhry, A., Rohrbach, M., Elhoseiny, M., Ajanthan, T., Dokania, P.K., Torr, P.H., Ranzato, M., 2019. Continual learning with tiny episodic memories .
- [13] Chen, T., Kornblith, S., Norouzi, M., Hinton, G., 2020. A simple framework for contrastive learning of visual representations, in: ICML.
- [14] Chen, Z., Liu, B., 2018. Lifelong machine learning. Morgan & Claypool Publishers.
- [15] Fei, G., Wang, S., Liu, B., 2016. Learning cumulatively to become more knowledgeable, in: Proceedings of the 22nd ACM SIGKDD International Conference on Knowledge Discovery and Data Mining, pp. 1565–1574.

- [16] Goodfellow, I.J., Shlens, J., Szegedy, C., 2015. Explaining and harnessing adversarial examples. ICLR .
- [17] Gummadi, M., Kent, D., Mendez, J.A., Eaton, E., 2022. Shels: Exclusive feature sets for novelty detection and continual learning without class boundaries, in: Conference on Lifelong Learning Agents, PMLR. pp. 1065–1085.
- [18] Han, K., Vedaldi, A., Zisserman, A., 2019. Learning to discover novel visual categories via deep transfer clustering, in: International Conference on Computer Vision (ICCV).
- [19] He, K., Zhang, X., Ren, S., Sun, J., 2016. Deep residual learning for image recognition, in: CVPR.
- [20] Hendrycks, D., Gimpel, K., 2016. A baseline for detecting misclassified and out-of-distribution examples in neural networks. arXiv preprint arXiv:1610.02136 .
- [21] Hendrycks, D., Mazeika, M., Kadavath, S., Song, D., 2019. Using self-supervised learning can improve model robustness and uncertainty, in: NeurIPS, pp. 15663–15674.
- [22] Henning, C., Cervera, M., D’Angelo, F., Von Oswald, J., Traber, R., Ehret, B., Kobayashi, S., Grewe, B.F., Sacramento, J., 2021. Posterior meta-replay for continual learning. Advances in Neural Information Processing Systems 34.
- [23] Hounsby, N., Giurigu, A., Jastrzebski, S., Morrone, B., De Laroussilhe, Q., Gesmundo, A., Attariyan, M., Gelly, S., 2019. Parameter-efficient transfer learning for nlp, in: International Conference on Machine Learning, PMLR. pp. 2790–2799.
- [24] Jafarzadeh, M., Dhamija, A.R., Cruz, S., Li, C., Ahmad, T., Boulton, T.E., 2021. A review of open-world learning and steps toward open-world learning without labels. arXiv e-prints , arXiv–2011.
- [25] Karakida, R., Akaho, S., 2022. Learning curves for continual learning in neural networks: Self-knowledge transfer and forgetting, in: International Conference on Learning Representations.



- [26] Ke, Z., Liu, B., Ma, N., Xu, H., Shu, L., 2021. Achieving forgetting prevention and knowledge transfer in continual learning. *Advances in Neural Information Processing Systems* 34.
- [27] Khosla, P., Teterwak, P., Wang, C., Sarna, A., Tian, Y., Isola, P., Maschinot, A., Liu, C., Krishnan, D., 2020. Supervised contrastive learning. *arXiv preprint arXiv:2004.11362* .
- [28] Kim, G., Esmaeilpour, S., Xiao, C., Liu, B., 2022. Continual learning based on ood detection and task masking, in: *CVPR 2022 Workshop on Continual Learning*.
- [29] Kirkpatrick, J., Pascanu, R., Rabinowitz, N., Veness, J., Desjardins, G., Rusu, A.A., Milan, K., Quan, J., Ramalho, T., Grabska-Barwinska, A., Others, 2017. Overcoming catastrophic forgetting in neural networks. *Proceedings of the National Academy of Sciences* 114, 3521–3526.
- [30] Krizhevsky, A., Hinton, G., 2009. Learning multiple layers of features from tiny images. *Technical Report TR-2009, University of Toronto, Toronto* .
- [31] Langley, P., 2020. Open-world learning for radically autonomous agents, in: *Proceedings of the AAAI Conference on Artificial Intelligence*, pp. 13539–13543.
- [32] Le, Y., Yang, X., 2015. Tiny imagenet visual recognition challenge.
- [33] Lee, K., Lee, K., Lee, H., Shin, J., 2018. A simple unified framework for detecting out-of-distribution samples and adversarial attacks. *Advances in neural information processing systems* 31.
- [34] Lee, K., Lee, K., Shin, J., Lee, H., 2019. Overcoming catastrophic forgetting with unlabeled data in the wild, in: *CVPR*.
- [35] Li, Z., Hoiem, D., 2016. *Learning Without Forgetting*, in: *ECCV*, Springer. pp. 614–629.
- [36] Liang, S., Li, Y., Srikant, R., 2018. Enhancing the reliability of out-of-distribution image detection in neural networks, in: *ICLR*. URL: <https://openreview.net/forum?id=H1VGkIxRZ>.

- [37] Liu, B., 2020. Learning on the job: Online lifelong and continual learning., in: AAAI.
- [38] Liu, B., Robertson, E., Grigsby, S., Mazumder, S., 2022. Self-initiated open world learning for autonomous ai agents, in: Proceedings of AAAI Symposium on ‘Designing Artificial Intelligence for Open Worlds’.
- [39] Liu, Y., Parisot, S., Slabaugh, G., Jia, X., Leonardis, A., Tuytelaars, T., 2020a. More classifiers, less forgetting: A generic multi-classifier paradigm for incremental learning, in: ECCV. Springer International Publishing, pp. 699–716.
- [40] Liu, Y., Su, Y., Liu, A.A., Schiele, B., Sun, Q., 2020b. Mnemonics training: Multi-class incremental learning without forgetting, in: CVPR.
- [41] Lopez-Paz, D., Ranzato, M., 2017. Gradient Episodic Memory for Continual Learning, in: NeurIPS, pp. 6470–6479.
- [42] Loshchilov, I., Hutter, F., 2016. Sgdr: Stochastic gradient descent with warm restarts. arXiv preprint arXiv:1608.03983 .
- [43] McCloskey, M., Cohen, N.J., 1989. Catastrophic interference in connectionist networks: The sequential learning problem, in: Psychology of learning and motivation. Elsevier. volume 24, pp. 109–165.
- [44] Ostapenko, O., Puscas, M., Klein, T., Jahnichen, P., Nabi, M., 2019. Learning to remember: A synaptic plasticity driven framework for continual learning, in: Proceedings of the IEEE/CVF Conference on Computer Vision and Pattern Recognition, pp. 11321–11329.
- [45] von Oswald, J., Henning, C., Sacramento, J., Grewe, B.F., 2020. Continual learning with hypernetworks. ICLR .
- [46] Pang, G., Shen, C., Cao, L., Hengel, A.V.D., 2021. Deep learning for anomaly detection: A review. ACM Computing Surveys (CSUR) 54, 1–38.
- [47] Parmar, J., Chouhan, S.S., Raychoudhury, V., Rathore, S.S., 2021. Open-world machine learning: Applications, challenges, and opportunities. arXiv preprint arXiv:2105.13448 .

- [48] Pentina, A., Lampert, C., 2014. A pac-bayesian bound for lifelong learning, in: International Conference on Machine Learning, PMLR. pp. 991–999.
- [49] Rajasegaran, J., Khan, S., Hayat, M., Khan, F.S., Shah, M., 2020. itaml: An incremental task-agnostic meta-learning approach, in: CVPR.
- [50] Ramanujan, V., Wortsman, M., Kembhavi, A., Farhadi, A., Rastegari, M., 2020. What’s hidden in a randomly weighted neural network?, in: Proceedings of the IEEE/CVF Conference on Computer Vision and Pattern Recognition, pp. 11893–11902.
- [51] Rebuffi, S.A., Kolesnikov, A., Lampert, C.H., 2017. iCaRL: Incremental classifier and representation learning, in: CVPR, pp. 5533–5542.
- [52] Russakovsky, O., Deng, J., Su, H., Krause, J., Satheesh, S., Ma, S., Huang, Z., Karpathy, A., Khosla, A., Bernstein, M., et al., 2015. Imagenet large scale visual recognition challenge. International journal of computer vision 115, 211–252.
- [53] Scheirer, W.J., Jain, L.P., Boult, T.E., 2014. Probability models for open set recognition. IEEE transactions on pattern analysis and machine intelligence 36, 2317–2324.
- [54] Schölkopf, B., Williamson, R.C., Smola, A.J., Shawe-Taylor, J., Platt, J.C., et al., 1999. Support vector method for novelty detection., in: NIPS, Citeseer. pp. 582–588.
- [55] Serra, J., Suris, D., Miron, M., Karatzoglou, A., 2018. Overcoming catastrophic forgetting with hard attention to the task, in: International Conference on Machine Learning, PMLR. pp. 4548–4557.
- [56] Shin, H., Lee, J.K., Kim, J., Kim, J., 2017. Continual learning with deep generative replay, in: NIPS, pp. 2994–3003.
- [57] Szegedy, C., Liu, W., Jia, Y., Sermanet, P., Reed, S., Anguelov, D., Erhan, D., Vanhoucke, V., Rabinovich, A., 2015. Going deeper with convolutions, in: CVPR. URL: <http://arxiv.org/abs/1409.4842>.
- [58] Tack, J., Mo, S., Jeong, J., Shin, J., 2020. Csi: Novelty detection via contrastive learning on distributionally shifted instances, in: NeurIPS.

- [59] Touvron, H., Cord, M., Douze, M., Massa, F., Sablayrolles, A., Jégou, H., 2021. Training data-efficient image transformers & distillation through attention, in: International Conference on Machine Learning, PMLR. pp. 10347–10357.
- [60] van de Ven, G.M., Tolias, A.S., 2019. Three scenarios for continual learning. arXiv preprint arXiv:1904.07734 .
- [61] Wortsman, M., R., V., Liu, R., Kembhavi, A., Rastegari, M., Yosinski, J., Farhadi, A., 2020. Supermasks in superposition, in: NeurIPS.
- [62] Wu, Y., Chen, Y., Wang, L., Ye, Y., Liu, Z., Guo, Y., Fu, Y., 2019. Large scale incremental learning, in: CVPR.
- [63] Xu, H., Liu, B., Shu, L., Yu, P., 2019. Open-world learning and application to product classification, in: The World Wide Web Conference, pp. 3413–3419.
- [64] Yan, S., Xie, J., He, X., 2021. Der: Dynamically expandable representation for class incremental learning, in: Proceedings of the IEEE/CVF Conference on Computer Vision and Pattern Recognition, pp. 3014–3023.
- [65] Yang, J., Zhou, K., Li, Y., Liu, Z., 2021. Generalized out-of-distribution detection: A survey. arXiv preprint arXiv:2110.11334 .
- [66] You, Y., Gitman, I., Ginsburg, B., 2017. Large batch training of convolutional networks. arXiv preprint arXiv:1708.03888 .
- [67] Zeng, G., Chen, Y., Cui, B., Yu, S., 2019. Continuous learning of context-dependent processing in neural networks. Nature Machine Intelligence .
- [68] Zenke, F., Poole, B., Ganguli, S., 2017. Continual learning through synaptic intelligence, in: ICML, pp. 3987–3995.
- [69] Zhu, F., Zhang, X.Y., Wang, C., Yin, F., Liu, C.L., 2021. Prototype augmentation and self-supervision for incremental learning, in: Proceedings of the IEEE/CVF Conference on Computer Vision and Pattern Recognition (CVPR), pp. 5871–5880.